THE GARRETT CORPORATION
AiResearch Manufacturing Division
LOS ANGELES 45, CALIFORNIA

N75-24743

(NASA-CR-132593) HYPERSONIC RESEARCH ENGINE PROJECT. PHASE 2A: INSTRUMENTATION PROGRAM Interim Technical Report, 24 Aug. - 23 Nov. 1967 (AiResearch Mfg. Co., Los Angeles, Calif.) 75 p CSCL 21E G3/07

Unclas 25370

REPORT NO. AP-67-3020

HYPERSONIC RESEARCH ENGINE PROJECT - PHASE IIA
INSTRUMENTATION PROGRAM
THIRD INTERIM TECHNICAL DATA REPORT
24 AUGUST THROUGH 23 NOVEMBER 1967
DATA ITEM NO. 55-8.03
NASA CONTRACT NO. NAS1-6665

AP 67-3020 21 December 1967

ISSUED MAY 1975

NO. OF PAGES 75

DATE 21 December 1967

PREPARED BY Engineering Staff

EDITED BY P. M. Parmar

APPROVED BY [signature]
Henry J. Lopez
HRE Program Manager

REVISIONS				ADDITIONS			
PAGE	DATE	PAGE	DATE	PAGE	DATE	PAGE	DATE

FOREWORD

This Interim Technical Data Report is submitted to the NASA Langley Research Center by AiResearch Manufacturing Company, a division of The Garrett Corporation, Los Angeles, California. The document was prepared in accordance with the guidelines established by paragraph 6.3.3.2 of NASA Statement of Work L-4947-B.

Interim Technical Data Reports are generated on a quarterly basis for major program tasks under the Hypersonic Research Engine Project. Upon completion of a given task effort, a Final Technical Data Report will be submitted.

The document in hand presents a detailed technical discussion of the Instrumentation Program for the period of 24 August through 23 November 1967.

ACKNOWLEDGMENTS

Acknowledgments for assistance in the completion of this document are extended to the following contributors:

N. Naves	Gas Sampling Probe and Double Sonic Orifice Probe
D. Osborn	Total Temperature Measurements
J. Pratt	Thrust/Drag System
G. Sawyer	Gas Analyzer
A. Vigilante	Overall Responsibility

CONTENTS

SYMBOLS

Symbol	Definition
a	$L_1/L = \frac{\text{distance between deflection block and parallel restraints}}{\text{distance between deflection block and rear supports}}$
α	angle of attack (airplane)
β	misalignment angle (error) - thrust block axis relative engine axis
γ	angle of deflection block flexure relative null position due to indicated thrust
Δ	deflection of block corresponding to indicated thrust
Δ_A	effective change of area of capacitor sensor due to thermal expansion
Δ_K	displacement of mid-point of bottom portion of block due to thermal expansion
Δ_F	force equivalent of effective change of area of capacitor
Δ_G	differential thermal expansion - engine to wishbone
Δ_H	displacement of mid-point of top portion of block due to thermal expansion
Δ_D	difference in depth of flexures due to moment on block M_B
Δ_L	increase in length of distance between block and rear supports due to thermal expansion
Δ_{L_1}	increase in length of distance between block and parallel restraints due to thermal expansion
Δ_T	displacement of thrust block (flexures) due to thermal expansion of engine/wishbone
Δ_x	effective displacement (along airplane axis due to rotation of capacitor centerplate under thermal expansion)
Δ_y	change in length of capacitor centerplate due to thermal expansion
Δ_o	change in length of capacitor outer plates due to thermal expansior
E	modulus of elasticity for deflector block material

SYMBOLS (Continued)

Symbol	Definition
e_1, e_2, e_3, e, e_a, e_b, e_c	absolute errors in measurands
f	vibration frequency
f_n	natural frequency of thrust/drag system (with engine)
$f_1(t) - g_1$	random vibration function - engine
$f_2(t) - g_2$	random vibration function - wishbone
F_B	vertical force in a flexure due to the moment M_B
F_A	force at thrust block due to actuator motion
$F_{K_1} - F_T$	force on deflection block due to differential thermal expansion - engine/wishbone
F_{K_2}	force on parallel restraints due to differential thermal expansion - engine/wishbone
F_{K_3}	force on rear supports due to differential thermal expansion - engine/wishbone
F_F	force along each flexure due to resolved vertical force at pin angle γ
F_M	force at deflection block equivalent to displacement under moment M_B
F_R	force at deflection block due to stiffness of parallel restraints and rear supports
F_Z	(maximum) aero. force on engine in Z axis

SYMBOLS (Continued)

Symbol	Definition
$g_1 = f_1(t)$	random vibration - engine
$g_2 = f_2(t)$	random vibration - wishbone
$G_1(f)$	power spectral density of vibration g_1
$G_2(f)$	power spectral density of vibration g_2
$H(f)$	gain factor wishbone/engine - across block (g_2 to g_1)
k_1	stiffness of deflection block (axially)
k_2	parallel restraint stiffness (axially)
k_3	rear support stiffness (axially)
L	distance between deflection block and rear supports
L_1	distance between deflection block and parallel restraints
L_2	distance between parallel restraints and rear supports
L_1^1	length of rear flexure under moment M_B
L_1^2	length of forward flexure under moment M_B
λ	angle of rotation of center plate relative to vertical axis due to thermal expansion
M_B	moment on block transferred through thrust pin
μ	coefficient of thermal expansion of block
μ_c	coefficient of thermal expansion of centerplate
μ_o	coefficient of thermal expansion of outer plates and support
n	roll-off index of random vibration g
$N_x = \ddot{X}$	aircraft axial acceleration
N_z	aircraft acceleration along Z axis
P	horizontal component of force in each flexure due to reaction and deflection angle γ

SYMBOLS (Continued)

Symbol	Definition
q	length of outer plates of capacitor
R_N	vertical force on thrust pin due to all forces and moments
σ	standard deviation (error analysis)
T	thrust block temperature - before engine firing
T_A	average temperature rise of block
T_1, T_2, T_3, T_4	thrust block temperatures
T_G	temperature gradient along block
T_{ind}	indicated thrust
T_{int}	internal thrust
θ	angle of pitch
w	width of center plate of capacitor
W	weight of engine
x	length of thrust block - between ℄'s of flexure
y	length of center plate of capacitor
$\bar{y}$	rms value of response of g_1 to g_2
ψ	angle of centerplate to vertical under moment M_b
Z	depth of thrust block
ξ	damping ratio of thrust system (mechanical)

1.0 SUMMARY

During the third interim reporting period, 24 August 1967 through 23 November 1967, the instrumentation program for the Hypersonic Research Engine (HRE) furthered the developments in each of the following categories:

- Thrust measurement
- Gas sampling
- Temperature measurement
- Pressure measurement
- System engineering

The following paragraphs describe the status of the principal categories of the HRE instrumentation development task after the third reporting period.

1.1 THRUST MEASURING SYSTEM

Further up-dating of the structural requirements, to provide a firm basis for design, has necessitated a revised stress analysis. This analysis and a heat transfer analysis are currently in progress. Vibration is still the major factor in the structural considerations of the thrust block, but it is anticipated that the temperature environment will not be as severe as previously considered, thus alleviating the thermal expansion problems and relaxing the requirements for the accelerometer.

The design of the other components remains basically unchanged.

1.2 GAS SAMPLING SUBSYSTEM

1.2.1 Gas Analyzer

Modification of the mass spectrometer that will be used to analyze the combustion gases H_2, H_2O, N_2, and O_2, has been completed. Experimental data shows that a step change in the composition of these gases at the entrance to a 60 ft inlet tube of the mass spectrometer will reach 99 percent of the final value within 2 to 5.5 per sec, when analyzing for H_2. Shorter times occur with the higher inlet pressures. An additional 1 to 1.5 sec are required when analyzing simultaneously for H_2O, N_2, and O_2. A light beam oscillograph was used to make measurements during the tests at ambient temperature with inlet pressure of 20, 30, and 50 psia.

A manual or automatic selection of the gas species is available. A switch allows the operator to select either manual or automatic operation.

The gas analysis system provides an analysis that is independent of the temperature and pressure of the gas sample entering the 60 ft inlet tube.

During the past quarterly reporting period, the gas analyzer was used in analyzing a Mach 3 gas sample of 16% helium and 84% nitrogen. The analysis showed the composition to be the same (±1/2%) as when the gas sample was flowing at nearly zero velocity.

1.2.2 Gas Sampling Total Pressure Probe

Fabrication of the initial probe is complete and fabrication of the backup probe is continuing. Testing of the first probe has been initiated and will continue upon completion of the 2 in. x 6 in. combustor installation at North American Rockwell. The probe has successfully completed all tests during this reporting period which include proof pressure, leak testing and low temperature supersonic flow tests with a known mixture ratio of bottled gases to verify that the probe can capture a representative sample of gases from a supersonic stream.

1.3 DOUBLE SONIC ORIFICE TOTAL TEMPERATURE PROBE

A device has been designed that will measure total temperature and pressure in the HRE combustor test rig and boilerplate engine by two independent methods. The two independent temperature measuring methods are the double sonic orifice technique and the calorimetric technique. The probe is designed such that it can traverse the gas flow stream on any axial plane without affecting the performance of the test rig in operation.

The analysis and detail design drawings for the probe have been completed including an error analysis.

Fabrication of the parts is approximately 90 percent complete and is continuing toward a completion date sometime after the initiation of the large scale combustor tests, allowing the probe to be introduced into the test program at a convenient time.

1.3.1 Total Temperature Thermocouple

The HRE Statement of Work requires that instrumentation shall be provided to determine the exhaust gas total temperature as one of the minimum requirements. A review of alternate methods of computing combustor efficiencies, however, indicates that unless the determined temperature is extremely accurate, the result would be largely indeterminate for this computation.

Figure 1.3-1 is a rough estimate of the percent error in equivalent chemical efficiency to the percent error in total temperature for two inlet total temperatures. The equivalent chemical efficiency is defined as the equivalent amount of fuel which is completely combusted to the total amount of fuel injected.

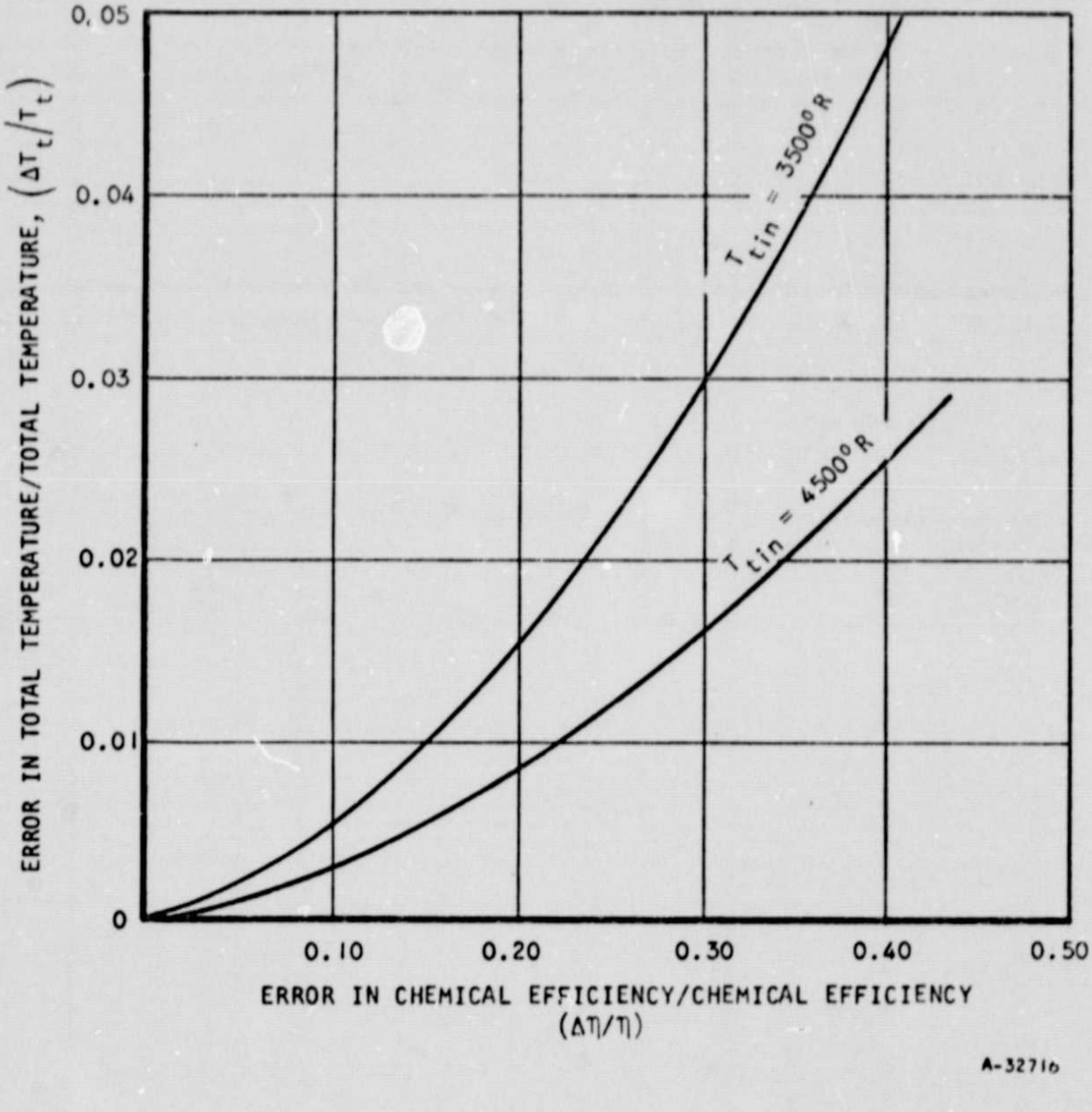

Figure 1.3-1. Estimate of Percent Error in Equivalent Chemical Efficiency to Percent Error in Total Temperature

For example, at Mach 8, one percent error in total temperature results in approximately 22 percent error in equivalent chemical efficiency at $\phi = 1$, or if 1.5 percent error of chemical efficiency is desired, the total temperature error must be within 0.1 percent. This stringent requirement is far beyond the state-of-the-art of high temperature measurement.

Another approach to determine the total temperature is from the thrust measurement. The I_{vac} at the exit can be computed from the indicated thrust, inlet momentum, additive drag, mass flow, pressure and viscous forces acting on the external surfaces (excluding wind shield) and the forces acting on the nozzle plug. Error analysis indicates that if the indicated thrust is 2.5 percent error, it results in an error of 3 percent in I_{vac}. Using this I_{vac}, the exit total temperature can be back-computed through I_{vac} charts in conjunction with flow rate and total pressure. Assuming that the total energy of the system is conserved, the estimated error in total temperature is 2 percent.

1.4 SYSTEM ENGINEERING

Effort has continued during the past reporting period to design the composite instrumentation system required for the first qualification engine. This instrumentation is composed of items for both flight and ground testing. The effort has concentrated on defining the system's requirements for accuracies, measurand locations and number, responses, environments and on determining the system's pattern with respect to transducer types, responses cable routing, and general concepts related to the instrumentation.

1% ERROR IN T_T = 22%
ERROR IN CHEM. EFFIC.

BEYOND STATE OF ART

2.0 THRUST/DRAG MEASUREMENT SYSTEM

2.1 PROBLEM STATEMENT

The objective of the thrust/drag measurement system is to determine the internal thrust developed by the engine during powered flight, and to determine the drag experienced during cold engine flight. To determine the engine's internal thrust, all extraneous loads due to drag, inertia, gravity, interface cabling, and fuel and coolant lines must be assessed. The active portion of the system is the deflection block. It forms part of the engine suspension system and therefore must withstand both inertial and aerodynamic loads and extremes of vibration, shock, and temperature.

Thrust will be measured calculating the deflection of a spring system. Both capacitive displacement and strain gauge methods will be evaluated to select the better indicating system. The measurement system must be able to operate in the following environments:

Force (over-range to 10,000 lb)	5000 lb drag to 7000 lb thrust
Temperature	-65^0F to $+400^0$F
Frequency response	0 to 10 cps

The revised thrust and drag force requirements are based on recent updated estimates.

The upper temperature limit has been relaxed to 400^0F (from 500^0F) as being a more realistic maximum (see Paragraph 2.4.3).

The system frequency response requirement of 0 to 10 cps is considered sufficient in the computation of the internal thrust. The previous upper limit of 100 cps was more applicable to the response of the deflection block with regard to mechanical considerations (see also Paragraph 2.4.2.6).

2.2 TOPICAL BACKGROUND

Several factors influence the design of the system. These factors are the varying aerodynamic and inertial forces arising from maneuvering flight conditions of the X-15 release, engine start and unstart, and landing. Since the deflection block forms one of the engine suspension parts, its structural integrity must be assured as must be the compatibility of the HRE with the dynamic loading and jettison capabilities of the X-15 airplane.

400^0F

Before the exact internal thrust can be computed, specific knowledge of external drag, frictional drag, aerodynamic drag, and resistance due to cabling fluid lines and additional engine suspension must be obtained as well as accurate determinations of temperature and suspension stiffness.

Internal thrust must be known to compute the specific impulse. The rate of fuel consumption must also be known. The allowable limit for error when the internal thrust is determined is partially governed by errors which may occur when the specific impulse is calculated.

The thrust block is subjected to extremes of temperatures which are dependent on conduction and radiation from the engine and from aerodynamically affected sources. Temperature is thus an important consideration in the selection of materials and components for the deflection block and the transducers associated with the thrust, drag, and inertial measurements which are close to the block.

2.3 OVERALL APPROACH

2.3.1 <u>Analytical</u>

The basic analytical approach remains the same as in previous Technical Data Reports and in Reference 1 but has been expanded to include all factors contributing to the indicated thrust reading. These factors are required to evaluate the internal thrust and to assess the error in this evaluation. Several are based on assumptions only and their contribution will be more accurately determined during development testing.

Figure 2.3-1 illustrates the factors considered and symbols used. The relationship of forces then becomes:

$$\underline{T_{INT} = T_{IND} + W\sin\theta + W_{\bar{x}} + D_E + F_R - F_T - F_I - R \pm g_I - F_E - F_M + \Delta_F}$$

(See Paragraph 2.4.2 for derivations)

The actuator force F_A is not included. Computation will use figures obtained during actuator inactivity.

Indicated thrust will be determined with a transducer, capacitive or strain gauge, which will measure the displacement in the direction of thrust from a block mounted between the engine and the airplane.

Aerodynamic drag force experienced during flight will be inferred from static pressure measurements and correlated with data obtained during the wind-tunnel engine testing phase.

Engine acceleration will be determined in flight with an accelerometer of suitable frequency response. This accelerometer will be mounted on the engine side of the deflection block.

The angle of pitch can be obtained from the X-15 readout instruments.

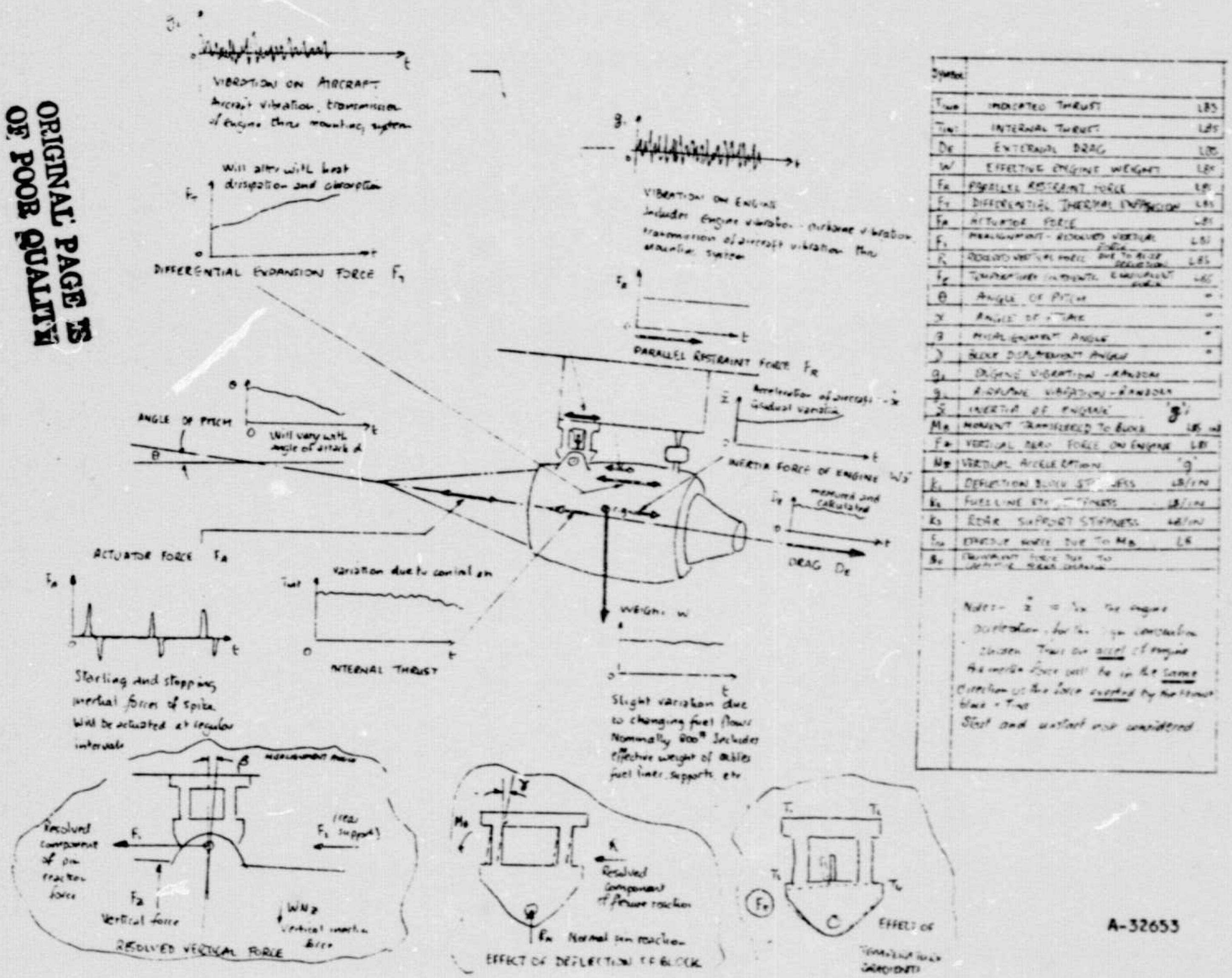

A-32653

Figure 2.3-1. Forces Acting on Thrust Block

2.3.2 Experimental

Full scale models of the deflection block and transducers will be subjected to a test program including the assessment of the effects of high and low temperatures, differential temperatures, dynamic and static characteristics, vibration under simulated engine loading, side loadings, and frequency response tests. These models will be fabricated from materials selected on structural and metallurgical bases and will incorporate both the capacitive displacement sensor and strain gauge sensors.

2.4 ANALYTICAL DESIGN

2.4.1 Analytical Design of the Deflection Block

The deflection block is the spring of a force measuring transducer and, at the same time one of the structural elements of the aircraft to ramjet interface.

Because of these multiple purposes, the following loads have been considered when designing the deflection block:

- Inertial
- Aerodynamic
- Thrust
- Vibration

Revision of the structural load requirements (Reference 4) and subsequent changes in the instrument range have necessitated a further stress analysis. A new problem statement has been issued to cover the later requirements. It contains a summary of the design factors as follows:

Reference	Factor	Value	Remarks
1	Maximum indicated thrust (measured)	7000 lb	Steady-state
2	Maximum thrust overload (test condition)	10,000 lb	Static test
3	Maximum indicated drag (measured)	5,500 lb	Steady state
4	Maximum drag overload (test condition)	7,500 lb	Static test

Reference	Factor	Value	Remarks
5	Deflection under condition I	0.003 in.	Linear
6	Temperature range (operational)	$-65^{0}F$ to $+400^{0}F$	May be revised as result of current heat transfer analysis
7	Temperature range (design)	$-65^{0}F$ to $+500^{0}F$	
8	Temperature gradient across block (max)	$200^{0}F$	Engine to wishbone
9	Temperature gradient along block (max)	$100^{0}F$	Along block
10	Axial stiffness of rear mounts	Zero	For design purposes
11	Cross axial stiffness of rear mounts (2)	0.25×10^{6} lb/in. (each) with respect to the engine ℄	(Including intermediate mounts)
12	Vibration (test condition)	10 cps to 31 cps ±0.03 in., 31 cps to 2000 cps 3 g	Consider as separate requirement. Magnification at resonance 6 to 1
13	Vibration (in flight)	10 to 2000 cps white noise PSD $0.018\ g^{2}/cps$ peaks to 3σ	Consider as complementary requirement. Magnification factor 6 to 1 at 200 cps, Roll-off above 200 cps at 12 db/octave
14	Landing shock	6.8 g normal -1 g transverse	
15	Landing vibration	---	Low frequency, high amplitude. High forces not involved
16	Flight conditions	See Reference 4	Cowl drag not acting on thrust block
17	Material for thrust block	Ti-6M-5V, Ni-Span-C	

?

17-4 PH

REVISED STRESS ANALYSIS IS IN PROGRESS

2.4.1.1 Stress Analysis

The revised stress analysis is presently in progress. As before, test vibration sinusoidal input (refer Statement of Work, Paragraph 4.6.2.1.1) is a governing factor in the flexure thickness and some redesign to give an effective larger length to thickness ratio and consequent lower stress has been suggested.

2.4.2 Derivation of Forces

The forces acting on the thrust block have been assessed with respect to their effect on the internal thrust calculation and their influence on the anticipated error in the calculation. The following derivations are made:

2.4.2.1 Resolved Vertical Force F_1-Due to Misalignment

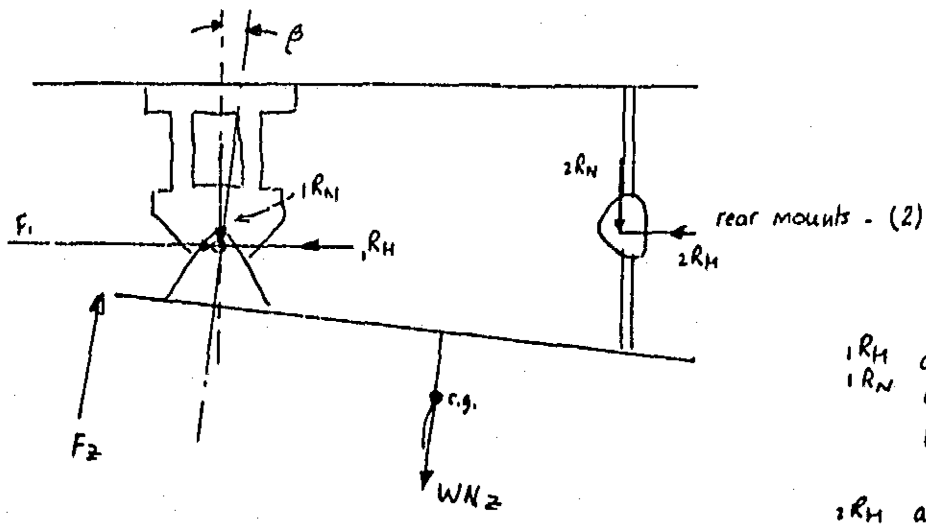

${}_1R_H$, ${}_1R_N$ are resolved components of the reaction at the thrust pin

${}_2R_H$, ${}_2R_N$ are the resolved components of the reactions at the rear supports.

Resolving horizontally $\quad {}_1R_H + {}_2R_M = (F_Z - WN_Z)\sin\beta$

Resolving vertically $\quad {}_1R_N + {}_2R_N = (F_Z - WN_Z)\cos\beta$

Since the thrust block is considerably stiffer in the horizontal direction than the rear supports ${}_2R_H$ can be approximated to zero.

Then

$${}_1R_H = (F_Z - WN_Z)\sin\beta$$

$$F_1 = -(F_Z - WN_Z)\sin\beta \qquad 1.1$$

Taking values

$F_Z = 754$ lb

$N_Z = 2.0$ g

$W = 800$ lb

$\beta = 1$ deg, max

giving

$\underline{F_1 = +14.7 \text{ lb}}$

2.4.2.2 <u>Force Due to Differential Thermal Expansion, F_T</u>

Differential thermal expansion between the wishbone and the engine will give rise to a deflection of the block and the rear support. Consider the following simplified spring system.

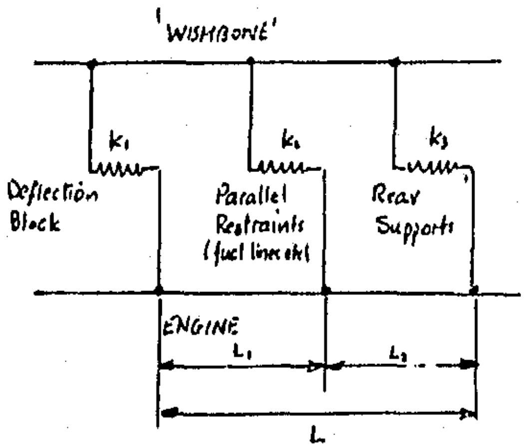

Let

F_{K_1} = force on deflection block

F_{K_2} = force on parallel restraints

F_{K_3} = force on rear supports

Δ_{L_1} = increase in length of L_1 due to thermal expansion

Δ_L = increase in length of L due to thermal expansion

Δ_T = displacement of deflection block

Equating forces

$$F_{K_1} = F_{K_2} + F_{K_3}$$

Therefore

$$K_1\Delta_T = K_2 \left(\Delta_{L_1} - \Delta_T\right) + K_3 \left(\Delta_L - \Delta_T\right)$$

$$\Delta_T \left(K_1 + K_2 + K_3\right) = K_2 \Delta_{L_1} + K_3 \Delta_L$$

$$\Delta_T = \frac{K_2 \Delta_{L_1} + K_3 \Delta_L}{K_1 + K_2 + K_3}$$

No Hysteresis Figured

If

$$K_1 >>> K_3 + K_2$$

and

$$L_1/L = a$$

Then

$$\Delta_T = \frac{\Delta_L}{K_1} \left[aK_2 + K_3\right] \quad 2.1$$

Force

$$F_{K_1} = \Delta_T K_1$$

$$F_{K_1} = F_T = \Delta_L \left[aK_2 + K_3\right] \quad 2.2$$

Assuming values

$\Delta_L = 0.1$ in.

$K_2 = 500$ lb/in. ← Total force for all fuel line, elect. connections, etc. ?

$K_3 = 1000$ lb/in. ← Resistance of pin at rear of wishbone ?

$a = 0.5$

Then

$$F_T = 125 \text{ lb}$$

Bad Assumptions

2.4.2.3 Resolved Vertical Force Due to Deflection of Thrust Block - R

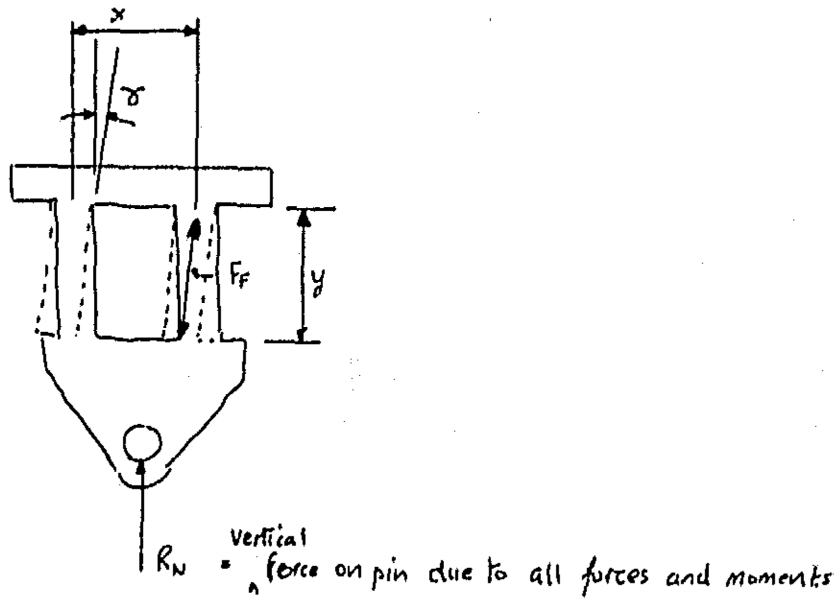

The force R_N will produce a compressive force F_F in each flexure. The horizontal component of this force will be P

$$P = F_F \sin \gamma$$

and

$$F_F = 1/2\ R_N/\cos \gamma$$

$$P = \frac{R_N}{2} \tan \gamma$$

Let the deflection under the load (horizontal) be Δ

then

$$\tan \gamma = \Delta/y$$

$$P = \frac{R_N}{2}\ \Delta/y$$

Now

$$\Delta = T_{ind}/K_1$$

where T_{ind} = indicated thrust

K_1 = flexure stiffness

Total horizontal force

$$\underline{R = 2P = \frac{R_N \; T_{ind}}{K_1 y}} \qquad 1.3$$

Assuming values

R_N requires computation from all forces and moments and is a variable of rear support position, inertia forces, internal thrust, etc. To give a typical value for R, R_N will be taken as 10,000 lb (based on previous stress analyses)

T_{ind}/K_1 = 0.003 in. (design)

y = 1.4 in. (present design)

$\underline{R = 21.4 \text{ lb}}$

2.4.2.4 Effect of Transferred Moment M_B

The effect of M_B will be to give uneven forces in each flexure

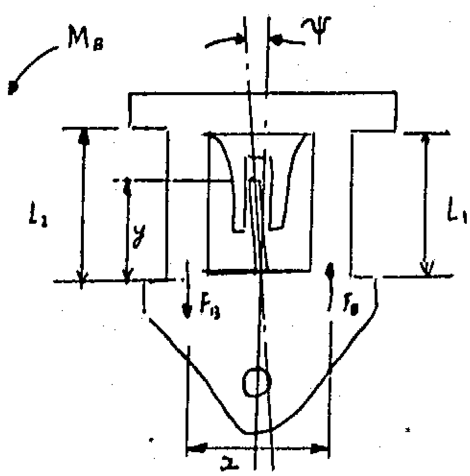

$L_2 - L_1 = \Delta_L$

$L_2 \doteq L_1 \doteq L$

$F_b x = M_B$; $F_b = M_B/x$

$\psi = \Delta_D/Z$

ORIGINAL PAGE IS OF POOR QUALITY

Mean displacement of center plate ·

$$D = y\psi/2$$

$$D = \frac{y\Delta_D}{2Z}$$

Now

$$\Delta_D = F_B/E$$

E = Young's modulus

$$D = \frac{F_b \cdot y}{2EZ}$$

Equivalent force F_M

$$F_M = \frac{F_b \cdot y\ K_1}{2EZ}$$

K_1 = block stiffness

or

$$F_M = \frac{M_B \cdot y\ K_1}{2E \times Z}$$

Assuming values

M_B = -500 lb in.

[based on applied moment -25,000 lb in. and coefficient of friction 0.02]

y = 1 in.

$K_1 = 2 \times 10^6$ lb/in.

$E = 16 \times 10^6$ (titanium), lb/in.^{2}

x = 2 in.

Z = 1.4 in.

$$F_M = \frac{500 \times 1 \times 2 \times 10^6}{2 \times 16 \times 10^6 \times 1.4 \times 2}$$

$$F_M = -11.2 \text{ lb}$$

F_M

2.4.2.5 Parallel Restraint Force F_R

The parallel restraints include fuel lines, electrical cables, and for the purposes of the derivation of F_R, also the rear supports (see 2.4.2.2)

$$F_R = \frac{K_2 + K_3}{K_1 + K_2 + K_3} \cdot T_{ind}$$

K_1 = deflection block stiffness

K_2 = stiffness of fuel lines, etc.

K_3 = stiffness of rear supports

Since

$$K_1 \gg K_2 + K_3$$

$$\underline{\underline{F_R = \frac{K_2 + K_3}{K_1} T_{ind}}} \qquad 4.1$$

Assuming values

K_2 = 500 lb/in.

K_3 = 1000 lb/in.

$K_1 = 2 \times 10^6$ lb/in.

T_{ind} = 6000 lb

F_R = 4.5 lb

2.4.2.6 Inertial Force and Vibration, $(W \cdot \ddot{x}, g_1)$

Weight W

The weight of the engine and accessories can be determined accurately. It must be included in the error analysis, however, due to the uncertainty of the effective weight-cable and piping clamping, variation of fuel flow. Nominal maximum effective weight is around 800 lb.

Acceleration $\ddot{x}$

The accelerometer provided will respond down to zero frequency and up to some defined upper frequency. It will thus respond to

Aircraft acceleration (Nx)

Vibration (g_i)

Variations in force (T_{ind})

There will also be cross-acceleration response from all directions (principally y and z axes).

The thrust block will also respond to the forces named above and it must be possible to eliminate the acceleration and vibration responses and leave the force variations.

Considering a frequency response of 0 - f cps for the accelerometer and a force variation of 10 percent max T_{ind}, then the peak acceleration associated with the force variation will be given by G where

$$G = cf^2D$$

where c = constant

D = displacement variation peak

$$G = cf^2 \times 0.1\ D_{max}$$

D_{max} = deflection of block under max indicated thrust

Typical Values

f = 10 cps

D_{max} = 0.003 in

c = 0.102

These yield G = 0.00307 g (compare with range of inertial acceleration 1 - 3g)

Vibration g_1

The vibration will be $g_1 = f_1(t)$ where $f_1(t)$ is a random function on the engine side of the block, and $g_2 = f_2(t)$, where $f_2(t)$ is a random function on the airplane side.

The thrust block will respond to the differential displacement and will be small at frequencies well below the system resonance and a maximum at resonance. The accelerometer, however, on the engine side of the block, will respond to the absolute acceleration of the engine, $g_1 = f_1(t)$ (vibration). Therefore direct cancellation of the vibration components are not possible. However, as will be shown, filtering on the outputs to below 10 cps will yield insignificant vibration data. The accelerometer will still need to handle this vibration signal unless the vibration is mechanically filtered.

Consider $g_2 = f_2(t)$ as an input to the system

let $g_1 = f_1(t)$ be the response of the system, taken as a single degree of freedom system, resonant frequency f_n, damping ratio ξ

let $G_1(f)$ be the power spectral density of the response

and $G_2(f)$ be the power spectral density of the input

then $G_1(f) = |H(f)|^2\, G_2(f)$, where $|H(f)|$ is the gain factor

$$|H(f)|^2 = \frac{1 + \left[2\xi \frac{f}{f_n}\right]^2}{\left[1 - \left(\frac{f}{f_n}\right)^2\right]^2 + \left[2\xi \frac{f}{f_n}\right]^2}$$

f = frequency

The total mean square value of the response $\bar{y}^2$ is given by

$$\bar{y}^2 = \int_0^\infty G_1(f)\, df$$

$$\bar{y}^2 = \int_0^\infty |H(f)|^2\, G_2(f)\, df$$

Substituting and integrating by the method of residues for <u>$G_2(f)$ constant</u>

$$\bar{y}^2 = \frac{\pi f_n (1 + 4\xi^2)\, G_2}{4\xi}$$

where G_2 = value of $G_2(f)$

If ξ is small compared to unity ·

$$\bar{y}^2 \approx \frac{\pi f_n \, G_2}{4\xi}$$

Typical values

$f_n = 150$ cps

$G_2 = 0.018\ g^2/\text{cps}$ (Statement of Work)

$\xi = 0.05$ (magnification of 10 to 1)

$\bar{y}^2 = 42.3\ g^2$

$\bar{y} = 6.5$ g

(note that the input 0.018 g^2/cps 20-2000 cps $\simeq$ 6.0 g rms)

This means that the accelerometer, if able to respond to the resonant frequency of the system, will have 6.5 g rms random acceleration signal in addition to the steady acceleration of approximately 2 g. The need to have as small a range as possible to reduce errors would present problems of overload and distortion.

Filtering on the input, by design of accelerometer, or mounting technique would remove this problem. The signal content below 10 cps would be quite small.

Assume 24db/octave roll-off below 20 cps from spectral density of 0.018 g^2/cps.

The rms value below 10 cps would then be [to 1 cps]

$$\sqrt{\frac{G_2 \ f_1}{n}\left[1 - \frac{1}{\left(\frac{f_2}{f_1}\right)^n}\right]}$$

where f_1 = lower frequency

f_2 = upper frequency

n = db/octave - 1

$$\text{rms value} = \sqrt{\left[\frac{0.018.1}{7}\left[1 - \frac{1}{(10)^7}\right]\right]}$$

rms value = 0.05 g

2.4.2.7 Deflection Block Thermal Expansion - F_E

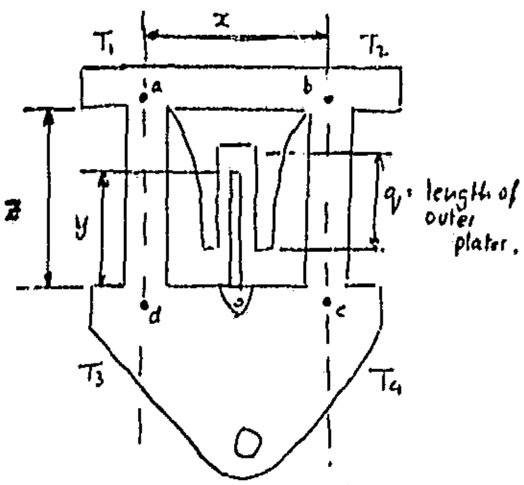

$T_3 > T_4 > T_1 > T_2$

$T_2 - T_1 = T_4 - T_3$

Ambient temperature = T (initial)

x, y, z at ambient

Consider the rectangle 'abcd' expanding under the temperatures T_1 T_2 T_3 T_4.

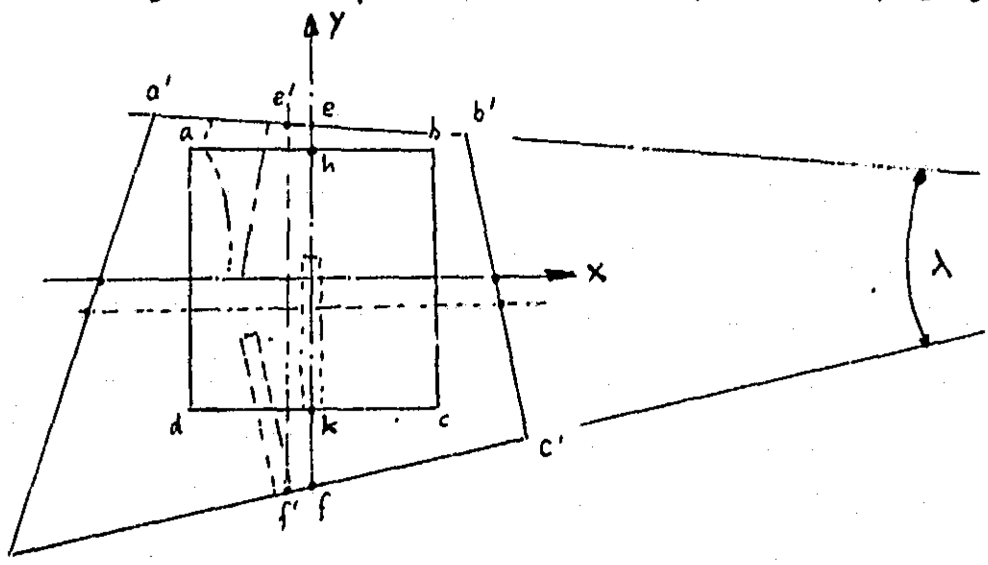

Each arm will expand linearly along its length

Consider the arm ab

Let temperature at midpoint h be T_5

Then displacement of h (in direction x) will be

$$\Delta h = \frac{1}{2}\left[\left(\frac{T_1 + T_5}{2} - T\right) - \left(\frac{T_2 + T_5}{2} - T\right)\right]\frac{\mu x}{2}$$

$$\Delta h = \frac{\mu x}{8}\,(T_1 - T_2)$$

μ = coefficient of expansion

If the displacements are small, each arm can be so treated, ignoring the effect of the non-squareness of a'b'c'd'.

then $\Delta_k = \frac{\mu x}{8}(T_4 - T_3)$

but $T_4 - T_3 = T_2 - T_1$

$\therefore \quad \Delta_k = \Delta h$

Thus the relative motion in the x (thrust) direction is confined to the rotation of the centerplate relative to the fixed capacitor plates. Another effect is the change in capacitor area (decrease).

x-direction relative motion (effective) = Δ_x

$$\Delta_x = \frac{y}{2} \sin \lambda$$

Very nearly

$$\sin \lambda = \frac{\Delta_{a'd'} - \Delta_{b'c'}}{c'd'}$$

$$\sin \lambda \approx \left(\frac{T_3 + T_1}{2} - \frac{T_2 + T_4}{2}\right) \frac{\mu Z}{x}$$

$$\sin \lambda = \frac{\mu Z}{x} \frac{1}{2} [(T_3 - T_4) + (T_1 - T_2)]$$

$$\sin \lambda = \frac{\mu Z}{x} [T_1 - T_2]$$

(since $T_3 - T_4 = T_1 - T_2$)

$\therefore$

$$\Delta_x = \frac{\mu Z y}{2x} [T_1 - T_2]$$

Equivalent force $F_E = \frac{\mu Z y}{2x} k_1 [T_1 - T_2]$

k_1 = block spring constant

Assuming values

$\mu = 5.1 \times 10^{-6}/^{\circ}F$

$Z = 1.4$ in.

$y = 0.9$ in.

$k_1 = 2 \times 10^6$ lb/in.

$x = 2$ in.

$T_1 - T_2 = 100^\circ F$ (assumed) [see Paragraph 2.4.3]

$$F_E = \frac{5.1 \times 1.4 \times 0.9 \times 100 \times 2}{2 \times 2} \text{ lb}$$

$$F_E = 320 \text{ lb}$$

Change of area

Let width of centerplate = w

Then change of effective area = $w[e'f' - hk] - w\Delta y - \frac{w\Delta_0}{2}$

where Δy = change in length of centerplate

Δ_0 = change in length of outer plate

Let change of area = Δ_A

$$\Delta_A = \left[\frac{a'd' + b'c'}{2} - Z - \Delta y - \Delta_0\right] w$$

$$\Delta_A = \left[\frac{\Delta_{a'd'}}{2} + \frac{\Delta_{b'c'}}{2} - \Delta y - \Delta_0\right] w$$

Let thermal expansion coefficient of centerplate = μ_c

and thermal expansion coefficient of outer plate (and support) = μ_o

then
$$\Delta_A = w\Big[\frac{1}{2}\left(\frac{T_1 + T_3}{2} - T\right)\mu Z + \frac{1}{2}\left(\frac{T_2 + T_4}{2} - T\right)\mu Z$$
$$- \left(\frac{T_1 + T_2 + T_3 + T_4}{4} - T\right)(\mu_c y + \mu_o q)\Big] \text{ approximately}$$

$$\Delta_A = w\left[\frac{T_1 + T_2 + T_3 + T_4}{4} - T\right][\mu Z - \mu_c y - \mu_o q]$$

The change in capacity will be directly proportional to the change in area; the effective force associated with such a change will be

$$\Delta_f = \frac{\Delta_A}{A} T_{ind}$$

A = area

$A = wy$ (approx.)

$$\Delta f = \frac{T_{ind}}{y}\left[\frac{T_1 + T_2 + T_3 + T_4}{4} - T\right][\mu Z - \mu_c y - \mu_o q]$$

Therefore, $\Delta f = \frac{6000}{0.9}[(250 - 100)(1.4 \times 5.1 - 2 \times 0.9)]\ 10^{-6}$

$\Delta f = 5.3$ lb

Assuming values

$T_{ind} = 6000$ lb	$T = 100^0F$
$y = 0.9$ in.	$\mu = 5.1 \times 10^{-6}/^0F$
$T_1 = 200^0F$	$\mu_c = 1 \times 10^{-6}/^0F$
$T_2 = 100^0F$	$\mu_o = 1 \times 10^{-6}/^0F$
$q = 0.9$ in.	$Z = 1.4$ in.
$T_3 = 400^0F$	$T_4 = 300^0F$

2.4.2.8 Indicated Thrust

The following figures are given

T_{int} = 5950 lb--up-to-date flight condition

$W = 800$ lb

$\theta = 8.8$ deg--up-to-date flight condition

$\ddot{x} = -2$ g--(aircraft acceleration -2 g)

$D_E = 699$ lb--up-to-date flight condition

$F_R = 4.5$ lb

$F_T = 125$ lb

$F_I = 14.7$ lb

$R = 21.4$ lb

F_E = 320 lb--latest heat transfer analysis will lower this figure (see Paragraph 2.4.3)

F_M = -11.2 lb

Δ_F = 5.3 lb

These yield

T_{ind} = 7189 lb

2.4.3 Heat Transfer Analysis

500°F

Heat transfer analysis is currently in progress. Preliminary results indicate that the temperature of the block will only reach 500°F at the pin locations and that gradients will be less than assumed. This would reduce the error due to differential block expansion (see 2.4.2.7) determination and allow the fitting of a standard temperature-range accelerometer.

2.4.4 Error Analysis

The error analyses so far conducted have been based on the relationship

$$T_{int} = T_{ind} + W \sin \theta + W\ddot{x} + D_E$$

Figures so established were published in References 1 and 2 and indicate a 3 σ error of ±3 percent in the internal thrust (Reference 2) and ±2.5 percent in the indicated thrust (Reference 1). However these errors were derived using different methods and with assumed parameter values which updating has changed. Consequently revised error analyses are necessary and should include the effect of the various factors discussed in the previous pages. The required accuracy of ±2.5 percent for the indicated thrust measurement is considered necessary to meet the requirement of determining the internal specific impulse to within 5 percent or better. It is important in stating these errors that they be defined and for the purposes of error analysis 3 σ errors are considered. Until the revised block design has been established and the heat transfer analysis considered, certain factors such as the differential thermal expansion of the block, cannot be truly assessed. Accordingly this report will show only the method of error analysis. The possible need to minimize errors in some of the contributory calculands by redesign or more critical measurement will be assessed after consideration of the detailed analysis and development testing.

2.4.4.1 Analysis Technique

2.4.4.1.1 Definition of Errors

Guarantee Maximum Error	No error will be greater than the guarantee maximum error
3σ Error	The probability is that 99.7 percent of all errors will lie between the limits $\pm 3\sigma$
Standard Error	$\pm 1\sigma$
Probable Error	$\pm 0.675\sigma$. The probability is that 50 percent of all errors will lie between the limits $\pm 0.675\sigma$

NOTES: (a) The probability errors are based on a random Gaussian distribution; σ = standard deviation (the 3σ error probability is applicable to other distributions)

(b) The guarantee maximum error should be at least a 6σ error

2.4.4.1.2 Measurand Error

The errors are randomly distributed about a common mean, namely the value of the measurand (there may also be a systematic error but this is determinate and is not included in the random assessment). The mean square method is used to sum the random errors as follows:

Let the contributory error be e_1 e_2 e_3.....etc.

Let the total error be e

then

$$e = \sqrt{e_1^2 + e_2^2 + e_3^2 + \ldots\ldots}$$

Since all errors have a common mean, they may be relative or absolute in the above relationship. They must all be similarly defined (e.g. 3σ)

2.4.4.1.3 Calculand Error

In this case the errors are not distributed about the required mean (true calculated value) but are distributed about the particular calculand mean. They must therefore be weighted in accordance with the effect of a small change in the calculand on the calculated value. For a given set of calculands it is unlikely that all errors will be at a maximum and rather will be randomly distributed. Applying this to a large number of sets of calculands, the errors will follow a random probability distribution. To determine the overall error a weighted root mean square method is used as follows:

Let P be a function of a, b, c, ...

$$P = f(a, b, c.....)$$

Let <u>absolute</u> error in P, a, b, c..... be e_p, e_a, e_b, e_c.....

Then

$$e_p = \sqrt{\left(e_a \cdot \frac{\partial p}{\partial a}\right)^2 + \left(e_b \cdot \frac{\partial p}{\partial b}\right)^2 + \left(e_c \cdot \frac{\partial p}{\partial c}\right)^2 + \ldots\ldots\ldots}$$

2.4.4.1.4 Application to Errors in Internal and Indicated Thrusts

The random error associated with a particular measurand, e.g. acceleration is obtained by reference to manufacturer's data, environment (e.g estimation of temperature and effect on thermal drift), instrument range, other associated equipment (power supplies), recording accuracy, etc. It is important to determine the error definition (guarantee probable 3σ). The individual measurand errors can then be combined using the relationship in Paragraph 2.4.4.1.3 to give the estimated overall error. Known or estimated values are used for the terms $\partial p/\partial a$. $\partial p/\partial b$ etc.

From Paragraph 2.3.1

$$T_{int} = T_{ind} + W \sin\theta + W\ddot{x} + DE + F_R - F_T - R - F_E - F_M + \Delta_F$$

Using the derivations covered under 2.4.2 this becomes

$$T_{int} = T_{ind}\left(1 + \frac{a - R_n}{K_1} + bT_A\right) + W(\sin\theta + \ddot{x} + cN_Z) - K_1(dM_b + T_G)$$

$$- (eF_Z + f\Delta_G)$$

where a,b,c,d,e,f are constants

R_N = normal block reaction

k_1 = block spring constant

T_A = average temperature rise of block

W = effective weight

θ = angle of pitch

$\ddot{x}$ = acceleration of airplane

N_Z = vertical acceleration

F_Z = vertical force

M_b = moment transferred to block

T_G = temperature gradient along block

Δ_G = differential thermal expansion between engine and wishbone

NOTES: (a) K_I will itself be a function of the block reaction R_N and decrease under a compressive load

(b) Some of the above terms are small and may be ignored in the error analysis eg T_{ind} . b T_A

(c) Also to be included in the error analysis are any errors introduced by the unknown portion of the vibration (see Paragraph 2.4.2.6)

2.4.5 Thrust Block Signal Conditioner

Minor circuit modification is envisaged to provide an attenuator in the output. This will reduce the maximum output signal to 15 mv to be compatible with the aircraft data recording system.

2.5 Future Action

The acceptance of a design to meet the latest structural and instrumental requirements will be followed by the fabrication of a development test block. Error and heat transfer analyses may influence the design and development testing will show the validity of some assumptions made in the instrument performance (e.g. temperature effects). A capacitor test block design will be completed in the near future. This block will form part of an assembly including the capacitor displacement transducer which will be used to evaluate the transducer and to provide a stable reference capacitor for developing the electronic signal conditioning equipment. Early tests will establish the structural integrity of the block and the dynamic behavior.

3.0 GAS SAMPLING SUBSYSTEM

The purpose of the gas sampling subsystem shown schematically in Figure 3.0-1, is to indicate the composition of the combustion gases. This subsystem is only to be used during ground tests in support ofthe 2 in. by 6 in. combustor development testing and Phase II boilerplate engine testing.

The gas sampling subsystem design effort is divided into two separate areas, (1) the analyzer and (2) the probe. Each is discussed in Paragraph 3.1 and 3.2, respectively. The analyzer determines the composition of the gas received from the probe. The probe is used to capture a representative sample of gas from the supersonic combustion stream, reduce its velocity to subsonic speeds, and feed a continuous sample into the analyzer.

3.1 ANALYZER

3.1.1 Problem Statement

The NASA Statement of Work requires an analysis of the gases captured by the gas sampling probe to determine the extent hydrogen mixes into the main air stream.

The analyses are to be restricted to hydrogen, oxygen, nitrogen, and water vapor with direct readouts in volume percent or sufficient information to calculate the volume percents.

3.1.2 Topical Background

The Hypersonic Research Engine Program requires an on-line gas analysis capability for supersonic combustion tests. To fulfill this requirement, a sample will be taken from a burning hydrogen and air mixture, cooled, and then analyzed for H_2, O_2, H_2O, and N_2 species which are expected to comprise at least 97 percent of the sample. From the resulting information, the atomic balance of hydrogen, nitrogen, and oxygen will be determined. It can then be determined if the hydrogen content increases due to hydrogen and air mixing in the combustor.

At the lowest temperature of the conditioned sample, free radical concentrations including NO, OH, H, O, and N, which are uncharged, are expected to be negligible. The gas analysis method described here will determine if the radical concentrations really are negligible at the low temperature.

Mixing information, derived from gas analysis, will be used as a parameter for determining combustor lengths.

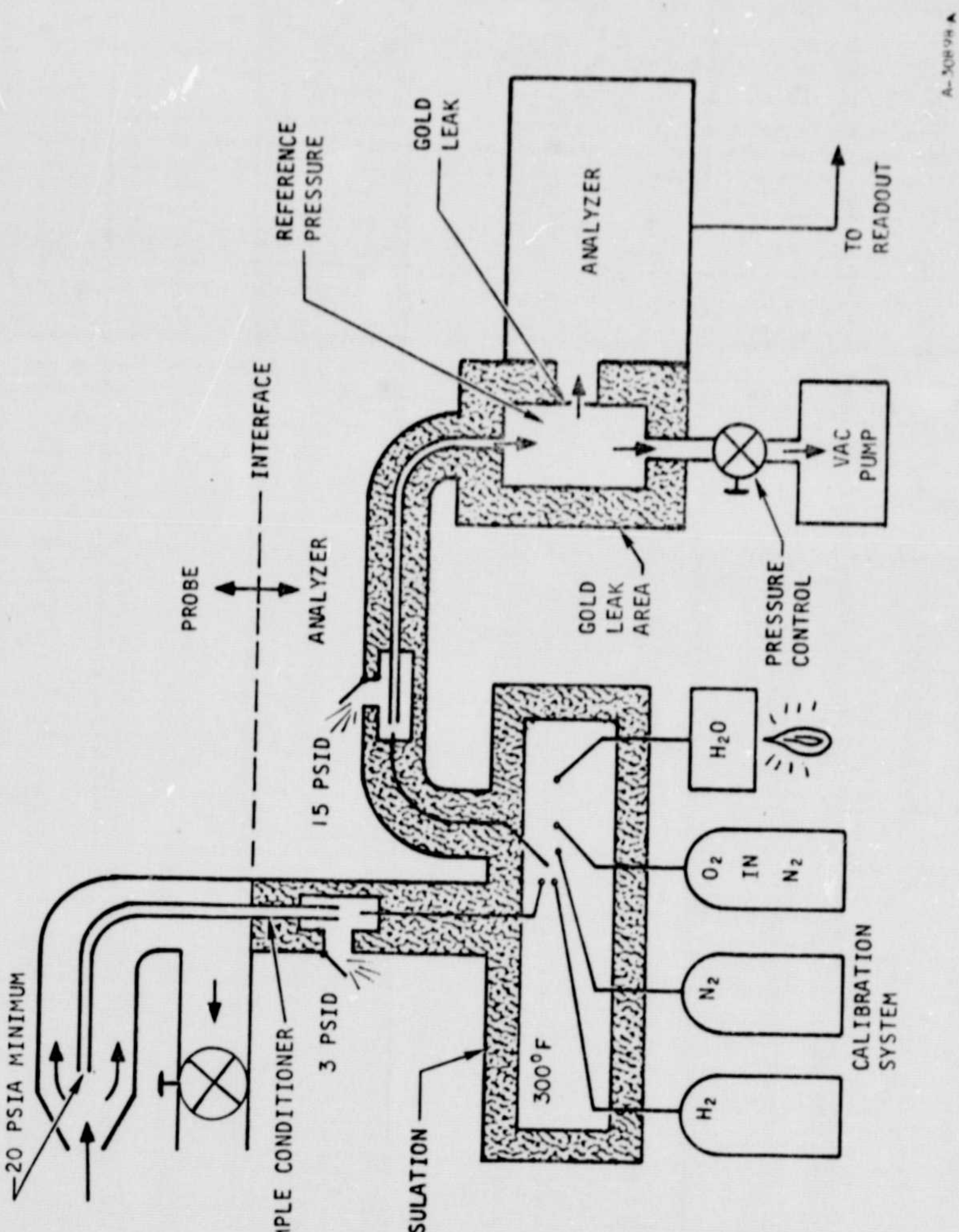

Figure 3.0-1. Gas Sampling Subsystem

ORIGINAL PAGE IS OF POOR QUALITY

3.1.3 Overall Approach

The percentage of O_2, N_2, H_2O, and H_2 will be measured. It might be possible to eliminate the N_2 measurement by making the assumption that the difference between 100 percent and the sum of O_2, H_2O, and H_2 is the percentage of N_2. If only three species were measured instead of four, a higher sampling rate could result. However, the procedure would force a synthetic total of 100 percent.

Every gas that would cause a deviation from a 100 percent total would require an explanation and an opportunity to discover errors. So, during the 2 in. by 6 in. combustor, and the Phase II boilerplate engine tests, all four gases will be measured as independent percentages with a mass spectrometer.

The mass spectrometer admits gas species, ionizes them, and sorts the ions on the basis of their mass-to-charge ratio. Figure 3.1-1 is a schematic of a mass spectrometer as it will be used in the combustor tests. Figure 3.1-2 and 3.1-3 show front and rear views of the mass spectrometer.

The mass spectrometer auxiliary cabinet is shown in Figure 3.1-4. The components of the auxiliary cabinet, identified from top to bottom, are as follows:

(a) Baratron pressure measuring device (for gold leak area)

(b) Baratron control panel (valving for pressure sensor)

(c) Peak selector panel

(d) Calibration gas selector

(e) Heater controls (to heat lines to prevent water vapor condensation)

(f) Vacuum pump (reference pressure for pressure sensor)

(g) Calibration system at combustor (not shown)

As shown in Figure 3.1-1, gas enters the capillary inlet at near ambient pressures and is pulled, by a vacuum pump, through the capillary tubes into the gold leak area. There, the pressure is reduced to about 2 mm Hg. The gold foil has 6 holes that are approximately 0.0004 in. dia. Gas travels through these holes into the ionizing region where uncharged molecules such as O_2 and N_2 are bombarded with a stream of electrons. This bombardment results in one or more electrons being stripped from the previously uncharged molecule resulting in a positively charged ion. This ion moves under the influence of static electric fields and the magnetic field of a permanent magnet. For any one value of an electric field, ions of only one mass-to-charge ratio can travel through the slits and arrive at the collector. Many ions piling up on the collector create a small current which is amplified and finally displayed on a recorder.

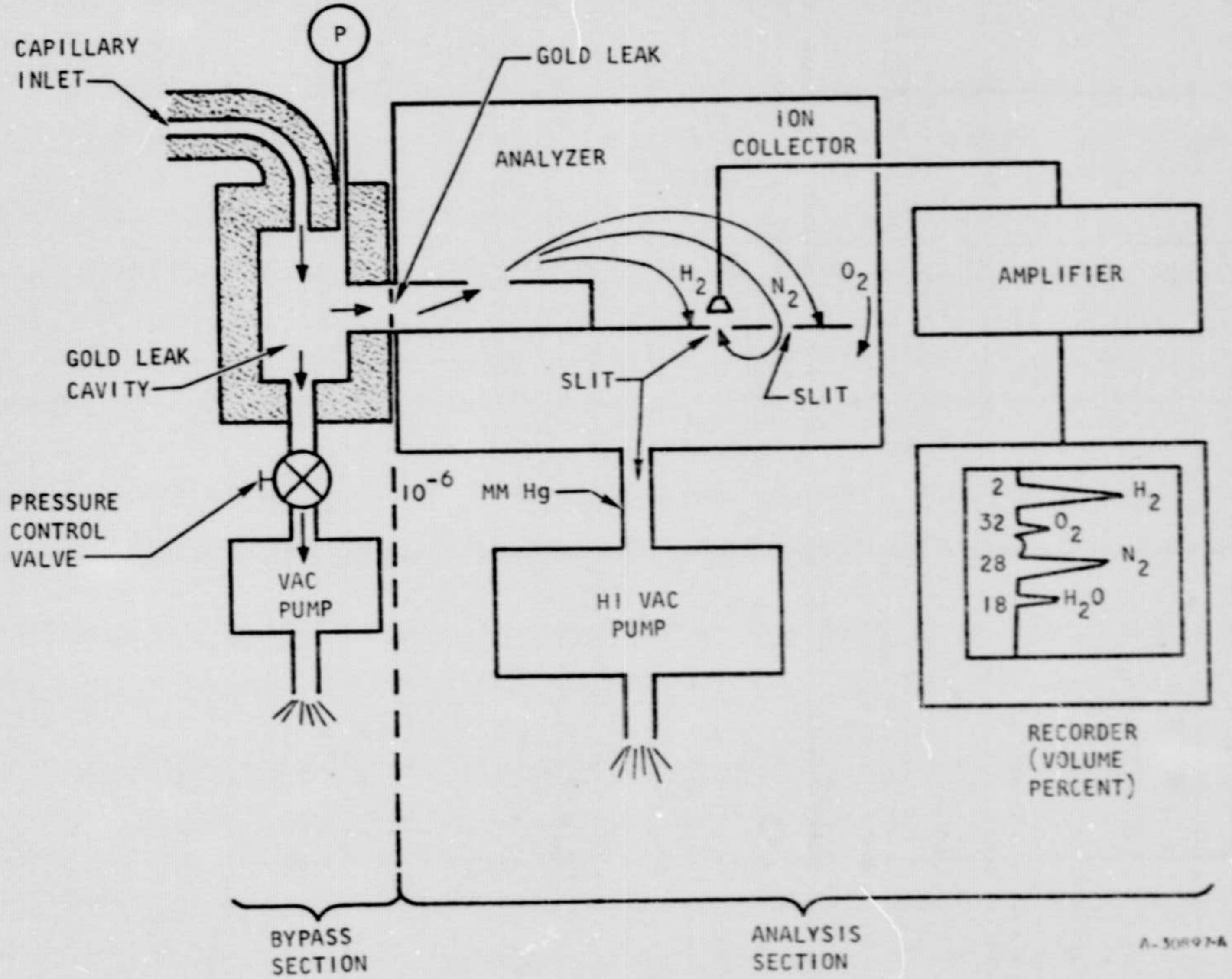

Figure 3.1-1. Mass Spectrometer, Schematic

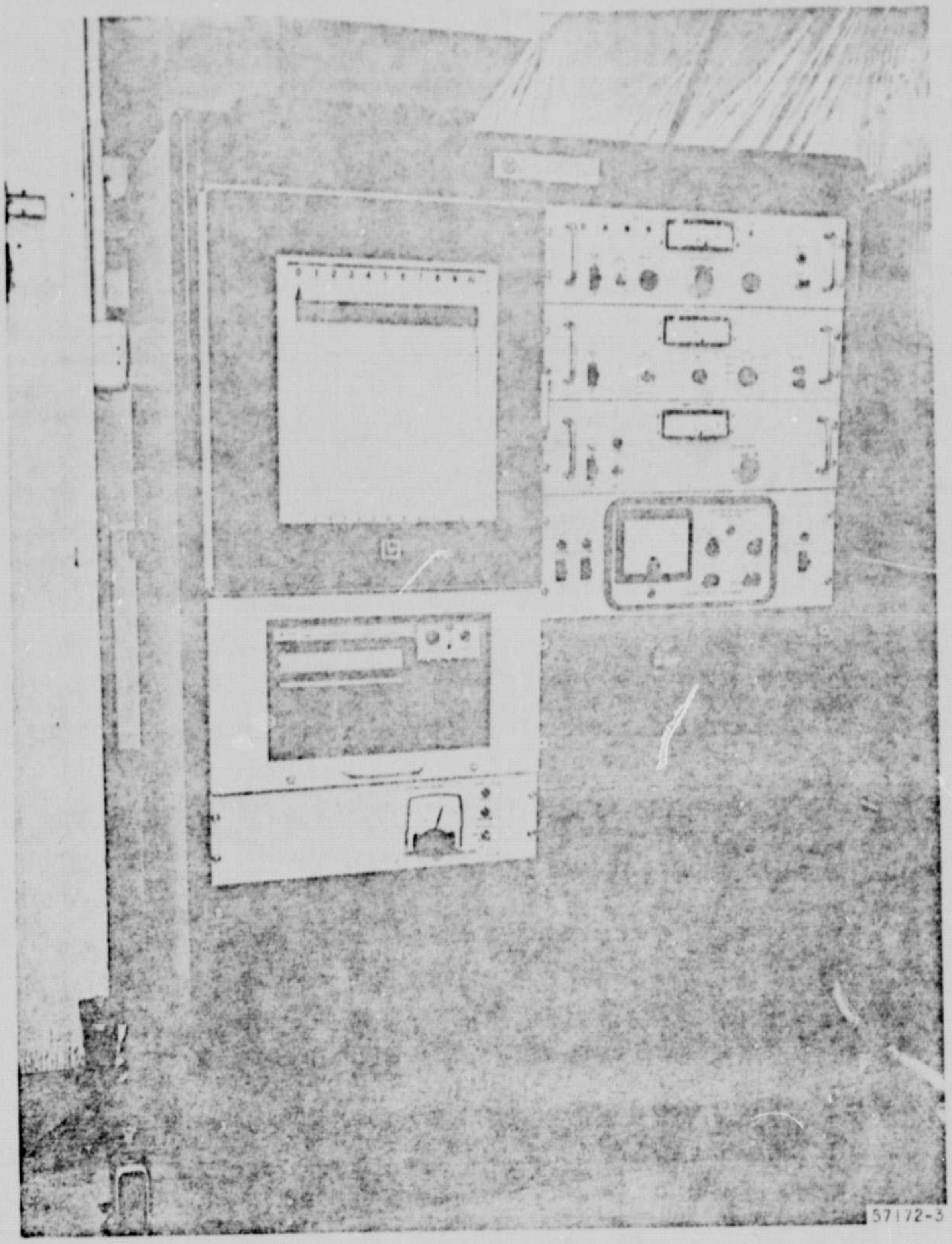

Figure 3.1-2. Mass Spectrometer (Front View)

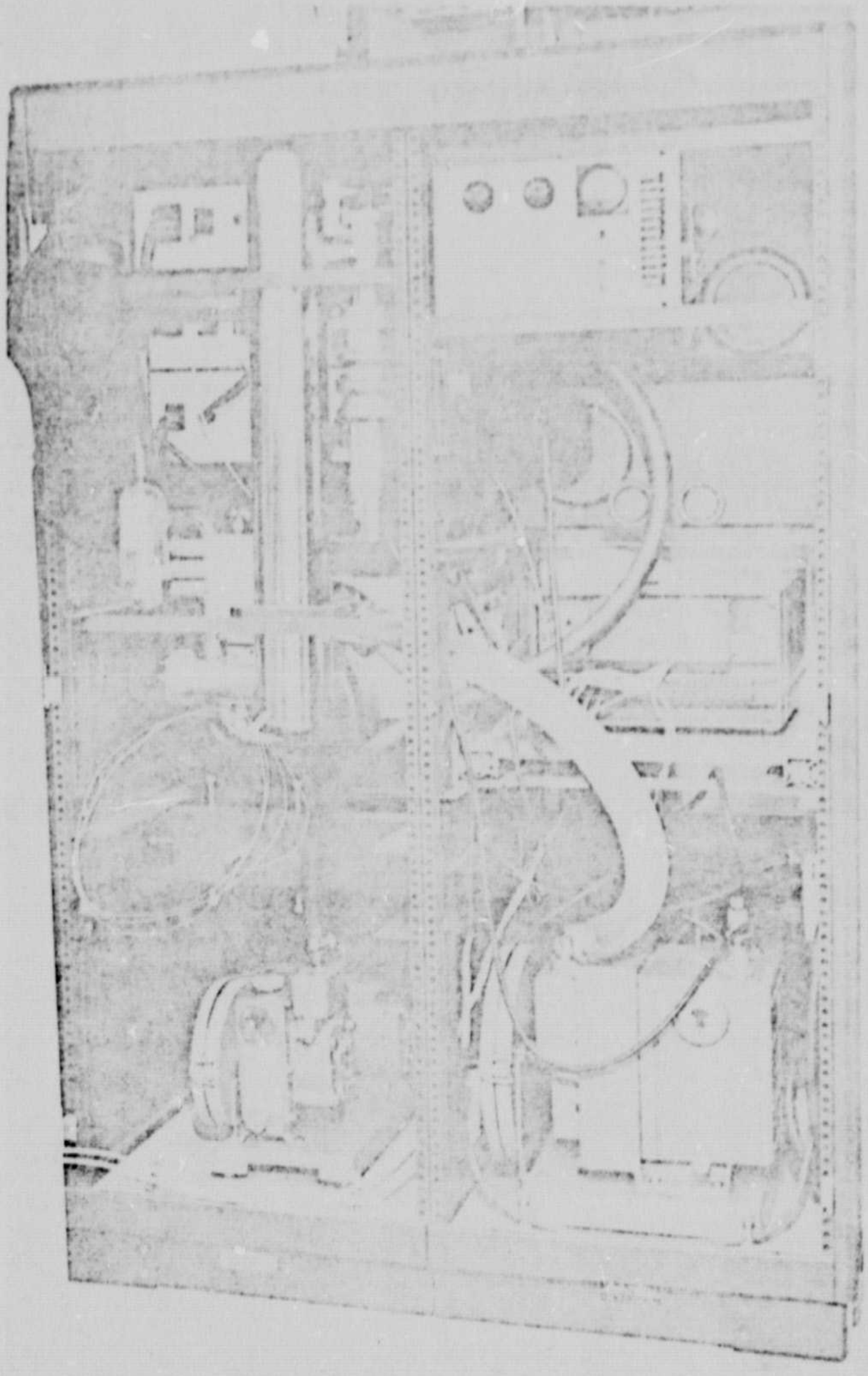

F-8152

Figure 3.1-3. Mass Spectrometer (Rear View)

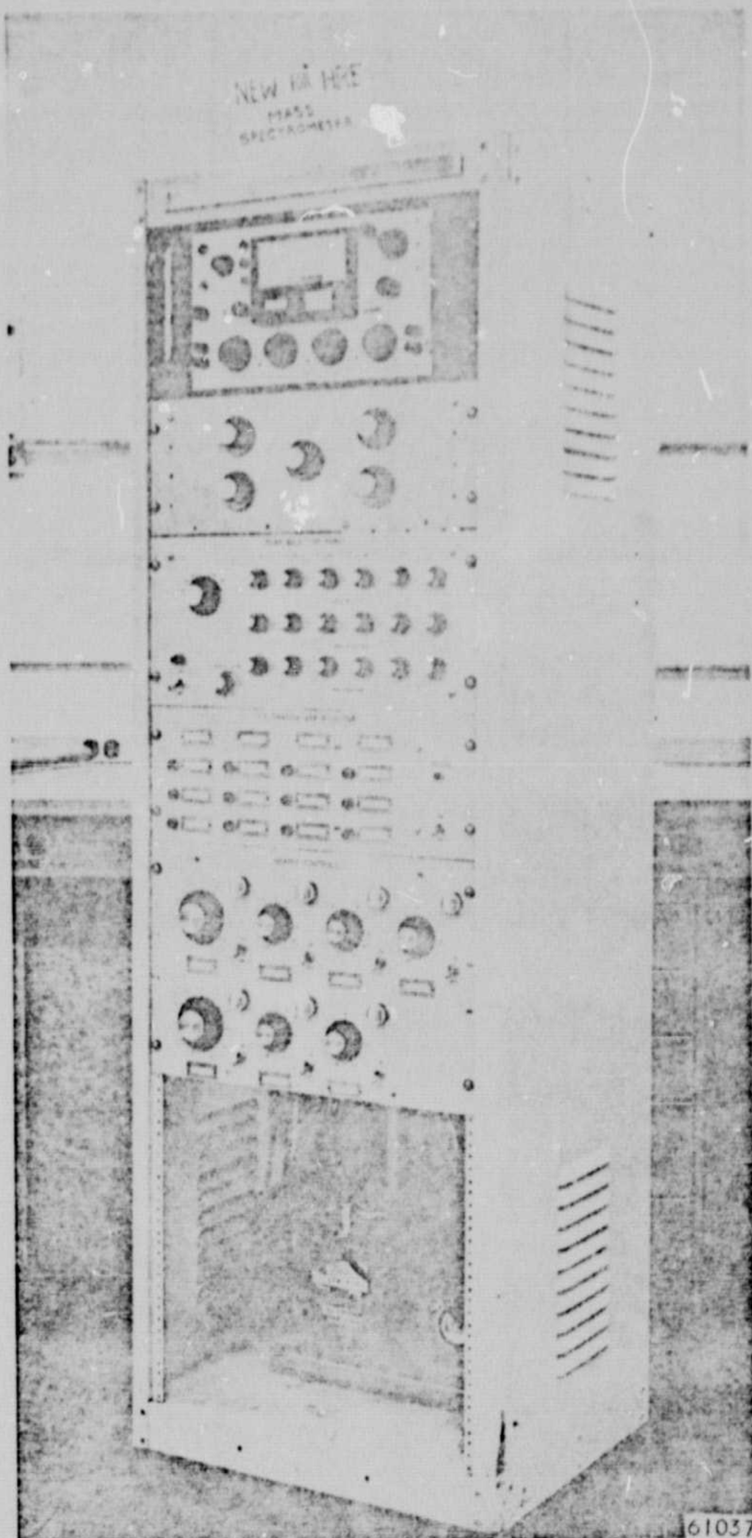

Figure 3.1-4. Mass Spectrometer Auxiliary Cabinet

The mass spectrometer was designed specifically to produce a continuous record displaying the composition of gas entering a 12 foot long capillary tube. The instrument rapidly responds to a step change in gas composition at the inlet to the capillary. The recorder may be calibrated to read in volume percent (same as mole percent at ambient pressure) the amount of any gas species. The instrument's sensitivity is very nearly the same for all gases. The record is easy to understand. For example, water vapor, with a molecular weight of 18, appears as 18, and nitrogen, with a molecular weight of 28, appears as 28.

The mass spectrometer can accurately measure the percentage of every stable gas. Also, the mass spectrometer, can determine the position of free radicals. The spectrometer's sensitivity may be estimated by assuming the sensitivity is similar to oxygen, nitrogen, or water vapor. At each position of free radicals, peaks may appear on the readout due to the presence of heavier molecules being fragmented or multiply charged.

3.1.4 Experimental Effort

3.1.4.1 Constant Conditions at Capillary Inlet

3.1.4.1.1 Mass Spectrometer Gas Consumption

The amount of gas (in cm^3 at ambient temperature and pressure) consumed by the mass spectrometer depends on whether 3 or 4 capillaries are used.

The gas consumption of the mass spectrometer, when 4 sections are used (sections 7, 8, 9, 10, Table 3.1-1), was experimentally determined to be 0.4 cm^3/sec when the gold leak pressure ranged between 1.1 and 50 mm Hg.

The gas consumption of the mass spectrometer when 3 sections are used (sections 8, 9, 10, Table 3.1-1) was experimentally determined to be 10.5 cm^3/sec when the gold leak pressure ranged between 8 and 50 mm Hg.

3.1.4.1.2 Gold Leak Pressure vs Ion Gauge Pressure

When the gold leak foil becomes plugged, the ionization gauge pressure drops. As an aid in determining whether the gold leak foil is plugged, which results in a drop in instrument sensitivity, values are given which were experimentally determined for a new gold leak foil. A plugged foil would produce lower ionization pressures for corresponding gold leak pressures than the ionization pressures shown. These values will be used as an index for future trouble shooting.

Gold Leak Pressure	Ion Gauge Pressure
1.0 mm Hg (0.04 in. Hg)	1.4×10^{-6} mm Hg
2.5 mm Hg (0.10 in. Hg)	3.0×10^{-6} mm Hg
5.0 mm Hg (0.2 in. Hg)	no data
23 mm Hg (0.91 in. Hg)	28×10^{-6} mm Hg

The mass spectrometer was designed specifically to produce a continuous record displaying the composition of gas entering a 12 foot long capillary tube. The instrument rapidly responds to a step change in gas composition at the inlet to the capillary. The recorder may be calibrated to read in volume percent (same as mole percent at ambient pressure) the amount of any gas species. The instrument's sensitivity is very nearly the same for all gases. The record is easy to understand. For example, water vapor, with a molecular weight of 18, appears as 18, and nitrogen, with a molecular weight of 28, appears as 28.

The mass spectrometer can accurately measure the percentage of every stable gas. Also, the mass spectrometer, can determine the position of free radicals. The spectrometer's sensitivity may be estimated by assuming the sensitivity is similar to oxygen, nitrogen, or water vapor. At each position of free radicals, peaks may appear on the readout due to the presence of heavier molecules being fragmented or multiply charged.

3.1.4 Experimental Effort

3.1.4.1 Constant Conditions at Capillary Inlet

3.1.4.1.1 Mass Spectrometer Gas Consumption

The amount of gas (in cm^3 at ambient temperature and pressure) consumed by the mass spectrometer depends on whether 3 or 4 capillaries are used.

The gas consumption of the mass spectrometer, when 4 sections are used (sections 7, 8, 9, 10, Table 3.1-1), was experimentally determined to be 0.4 cm^3/sec when the gold leak pressure ranged between 1.1 and 50 mm Hg.

The gas consumption of the mass spectrometer when 3 sections are used (sections 8, 9, 10, Table 3.1-1) was experimentally determined to be 10.5 cm^3/sec when the gold leak pressure ranged between 8 and 50 mm Hg.

3.1.4.1.2 Gold Leak Pressure vs Ion Gauge Pressure

When the gold leak foil becomes plugged, the ionization gauge pressure drops. As an aid in determining whether the gold leak foil is plugged, which results in a drop in instrument sensitivity, values are given which were experimentally determined for a new gold leak foil. A plugged foil would produce lower ionization pressures for corresponding gold leak pressures than the ionization pressures shown. These values will be used as an index for future trouble shooting.

Gold Leak Pressure	Ion Gauge Pressure
1.0 mm Hg (0.04 in. Hg)	1.4×10^{-6} mm Hg
2.5 mm Hg (0.10 in. Hg)	3.0×10^{-6} mm Hg
5.0 mm Hg (0.2 in. Hg)	no data
23 mm Hg (0.91 in. Hg)	28×10^{-6} mm Hg

TABLE 3.1-1

INLET TUBE SYSTEM DETAILS

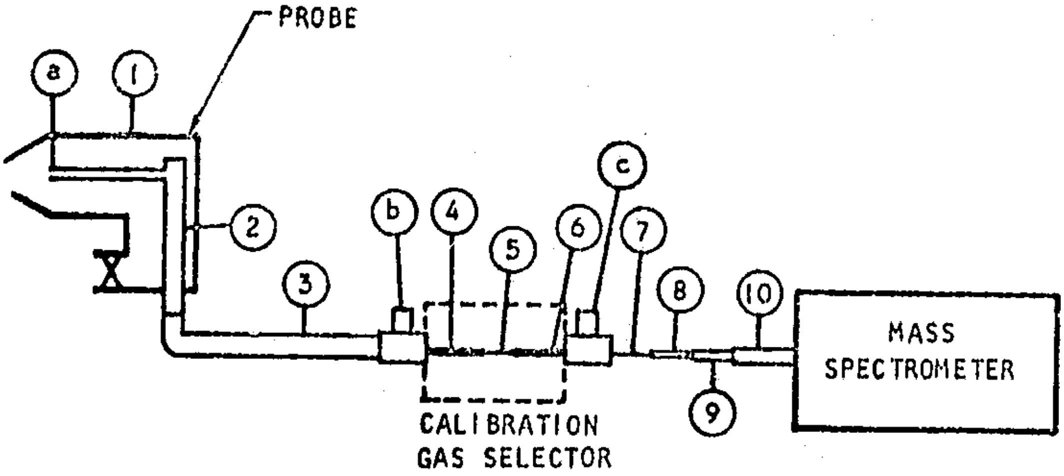

TUBING DETAILS

Tube No.	Inside Diameter, Mils	Length, ft	Gas Temperature, °R
1	72	1	3650
2	238	1	1560
3	120	30	860
4	62	1	735
5	32	0.17	735
6	62	1	735
7	13	5.1	685
8	27	5.8	685
9	55	6.3	685
10	101	5.2	685

Position Description

(a) Input to gas sampling tube
(b) 3 psia relief valve (P - 17.7 psia max)
(c) 0.15 psia relief valve (P = 14.85 psia max)
(d) 0.2 psia pressure at mass spectrometer gold leak

3.1.4.2 Variable Conditions at Capillary Inlet

3.1.4.2.1 Quantity of Gas Provided by Inlet System

The pressure at point "a" Table 3.1-1 must be high enough to force enough gas through the tubing and out tube 6 to provide the mass spectrometer with the gas it consumes. Depending on whether tube 7 is used or not the consumption of the mass spectrometer is 0.4 or 10.5 cm^3/sec. The gas flow from tube 6 was experimentally determined for various pressures at "a." Results are shown in Table 3.1-2. This table shows that the pressure at "a" must be slightly higher than 1 psig to supply 10.5 cm^3 to the mass spectrometer. If the pressure is less than this, a partial vacuum will exist within the tubing upstream of tube 7. Leaks in the system will then degrade the analysis of the gas sample from the probe because air will dilute the sample.

Experiments may be done to determine the effects of leaks on the analysis when the pressure at "a" is less than one atmosphere.

The inlet system shown in Table 3.1-1 was simulated except that tube 3 was 40 rather than 30 feet long.

The pressure P_2 indicates pressure (psig) at the point where tubes 2 and 3 join. The purpose of removing tube 7 would be to decrease the transport time of the gas sample.

TABLE 3.1-2

QUANTITY OF GAS AVAILABLE TO
THE MASS SPECTROMETER FOR VARIOUS INLET PRESSURES

Pressure at "a" (Table 3.1-1)	P_2	Gas Flow
1 psig	1 psig	10 standard cm^3 per sec
5 psig	4.5 psig	35 standard cm^3 per sec
9.5 psig	8 psig	----
20 psig	15.5 psig	----
40 psig	32 psig	----
70 psig	55.5 psig	55 standard cm^3 per sec

3.1.4.2.2 Choice of Operating Pressure at Gold Leak

In choosing the nominal operating pressure at the gold Leak (Figure 3.0-1) the following considerations are of importance, (1) the pressure should be easily controlled by the operator, (2) the pressure should be as high as possible so a large output is obtained, and (3) the linearity of the instrument should be such that the sum of the species is adequately close to 100 percent.

(a) The pressure should be easy to control.

The following experimental data was obtained.

Gold Leak Pressure	
1 mm	extremely easy to control
2.5 mm	very easy to control
23 mm	difficult to control

(b) The pressure should be as high as possible to provide a large output.

(c) The linearity of the instrument should be such that the sum of the species is adequately close to 100 percent.

Gold Leak Pressure	Hydrogen, Percent	Nitrogen, Percent	Total, Percent
1 mm Hg	23.8	76.2	100
2.5 mm Hg	23.6	76.2	99.8
5.0 mm Hg	22.6	76.8	99.4
23.0 mm Hg	18.7	79.9	98.6

(d) The output divided by gold leak pressure should be constant over a pressure range of ±50 percent of the nominal operating pressure. This data has not yet been obtained, but is expected to become worse as the pressure increases.

On the basis of the data that was obtained, the nominal operating pressure at the gold leak has been chosen to be 2.5 mm Hg.

3.1.4.2.3 Sensitivity of Gold Leak Pressure to Probe Pressure

The inlet system was designed to result in little fluctuation of pressure at the gold leak (which would yield a nearly constant output at the recorder) when the inlet pressure at the probe point "a" (Table 3.1-1) varied over a considerable pressure range. Test data showed that when the pressure at "a" varies from 5 psid to 100 psid, the gold leak pressure changes by 0.2 percent. Thus, the gold leak pressure is essentially insensitive to probe pressure.

3.1.4.2.4 Sensitivity of Gold Leak Pressure to Gas Composition Entering Probe

The pressure at the gold leak, however, changes when the gas composition changes that enters "a". The inlet pressure of gas in all cases is one atmosphere.

Composition of Gas Entering "a"	
100% N_2	5 mm reference pressure
76% N_2 24% H_2	down 7% from reference pressure
100% H_2	down 26% from reference pressure
100% O_2	down 2.3% from reference pressure
100% He	down 46% from reference pressure

Thus, the gold leak pressure is composition sensitive.

3.1.4.2.5 Output Linearity vs Gold Leak Pressure

In order to increase the instrument output, it is desirable sometimes to increase the gold leak pressure. However, when this is done, the output linearity changes at least for the gold leak used prior to serial number 35546. Data was not taken on serial number 35546. The test was performed on October 9, 1967.

Gold Leak Pressure mm Hg	Divisions Output	Divisions per mm Hg
2	265	132.5
3	396	132.0
5	667	135.4
10	1343	134.3
20	2738	136.9
30	4126	137.5

This shows that a 4 percent output error will result if the sensitivity at 3 mm Hg is used for calibration, a 30 mm Hg pressure is used for a test, and only a factor of 10 is considered in normalizing the test data to a 3 mm gold leak pressure.

3.1.4.3 Sensitivity of Mass Spectrometer

The sensitivity of the mass spectrometer (C-17852) depends on several variables. The data given is for the mass spectrometers output being recorded on the L & N ink pen recorder. One division represents 0.1 inch on the recorder.

Divisions	10,000 (100 at attenuation = 100)
Ionization current	20 microamperes
Gold leak pressure	5 mm Hg
Gold leak conductance	0.02 cm^3/sec
Serial number	35546 (CEC)
Number of holes	6
Ionization gauge pressure	5.8×10^{-6} mm Hg
Date performed	November 2, 1967

3.1.5 Future Action

3.1.5.1 Heating Equipment

Installation and checkout of the heating equipment for the pneumatic selector switch, sample conditioner and lines to the pressure sensor and to the water vaporizer, with appropriate thermal insulation, is in progress.

3.1.5.2 Temperature Monitoring

The temperature of all heated areas will be monitored. Thermocouples will be used for sensing temperature. The read out device may be a Leeds and Northrup indicator with push button selection for as many as 24 channels. This work is in progress.

3.1.6 System Checkout

Checkout of the analyzer system will be continued using gases of known composition; the temperatures, pressures, flows and compositions of the gases at the analyzer inlet being determined by the probe.

The entire gas sampling subsystem should be tested under conditions simulating at least some of the conditions that will occur during the combustor tests. Two types of gas mixtures are of interest. One type is molecularly mixed gases in which the heavy gas molecules and light gas molecules are homogeneously mixed. The second is turbulently mixed gases in which the heavy gas molecules and light gas molecules are not homogeneously mixed; some zones being richer in heavy gas than light gas and vice-versa. The molecularly mixed case is the simpler of the two cases.

However, a test was performed to determine the ability of the gas sampling subsystem to accurately determine the volume percents of helium and nitrogen in a molecularly mixed gas mixture. The mixture was 16 percent helium and 84 percent nitrogen. These gases were discharged through a Mach 3 nozzle and the gas sampling probe tip was placed in the Mach 3 gas stream; the temperature was ambient.

The test was conducted in order to find out if the gas subsystem indicates the same composition when sampling the mixture at a Mach 3 velocity, using the gas sampling probe, as when sampling that same mixture at nearly zero velocity, not using the gas probe. The test setup used is shown schematically in Figure 3.1-5, "Schematic of Mach 3 Test of Gas Sampling Subsystem." The composition of the gas was recorded before and after the test. The results are tabulated below:

TABLE 3.1-3

GAS COMPOSITION AT MACH 3

Test Description (See Figure 3.1-6)	Settling Chamber Pressure	Sample Line	Composition of Gas Sample	Total
Pre-Test	15 psig	A	16.5% He, 84% N_2	100.5%
Test (using probe)	500 psig	B	16.5% He, 83.5% N_2	100%
Post-Test	15 psig	A	16.0% He, 83.5% N_2	99.5%

Helium was used instead of hydrogen because of safety considerations.

The Pre-Test, Test, and Post-Test records are shown in Figure 3.1-6, "Records of Mach 3 Test of Gas Sampling Subsystem." Photographs of the test setup are shown in Figures 3.1-7, -8, -9. A drawing of the nozzle is shown in Figure 3.1-10.

The composition of the gas as analyzed by the vendor was 15.0 ±0.1 percent. The difference between the analysis made by the vendor and the analyses made by the writer has not been resolved. This may be done in the future, but is not required for fulfilling the purposes of this test. The purpose of this test was to compare the analysis taken by the probe at Mach 3 with the analysis taken at essentially zero velocity. The sample taken at zero velocity was taken from sample line A, Figure 3.1-9. It should be noted however, that the composition of helium and of nitrogen were independently determined by the writer. By considering only the helium or only the nitrogen, the helium percentage is 16 percent. Also, when adding He and N_2, the total ranges between

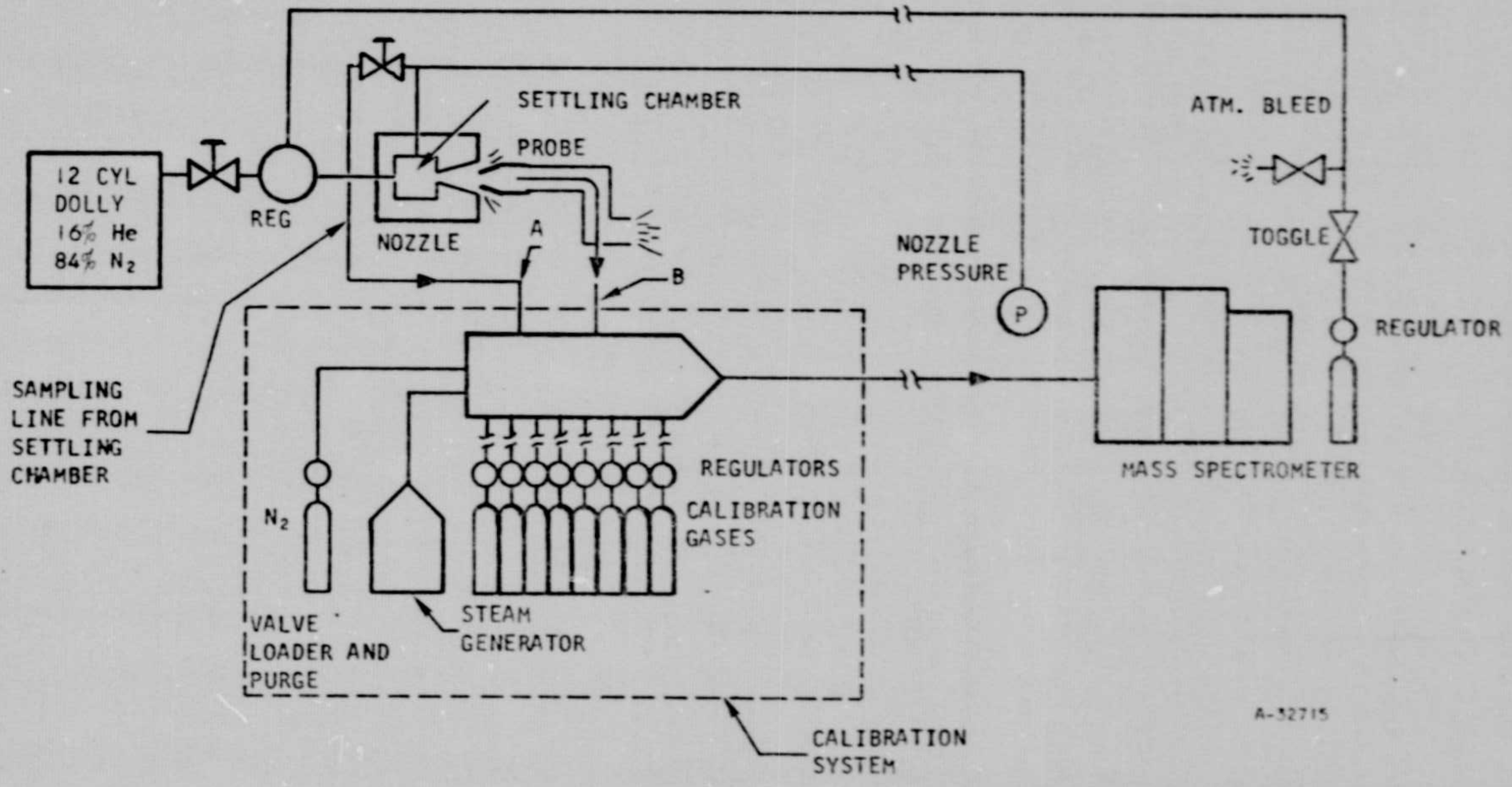

Figure 3.1-5. Schematic of Mach 3 Test of Gas Sampling Subsystem

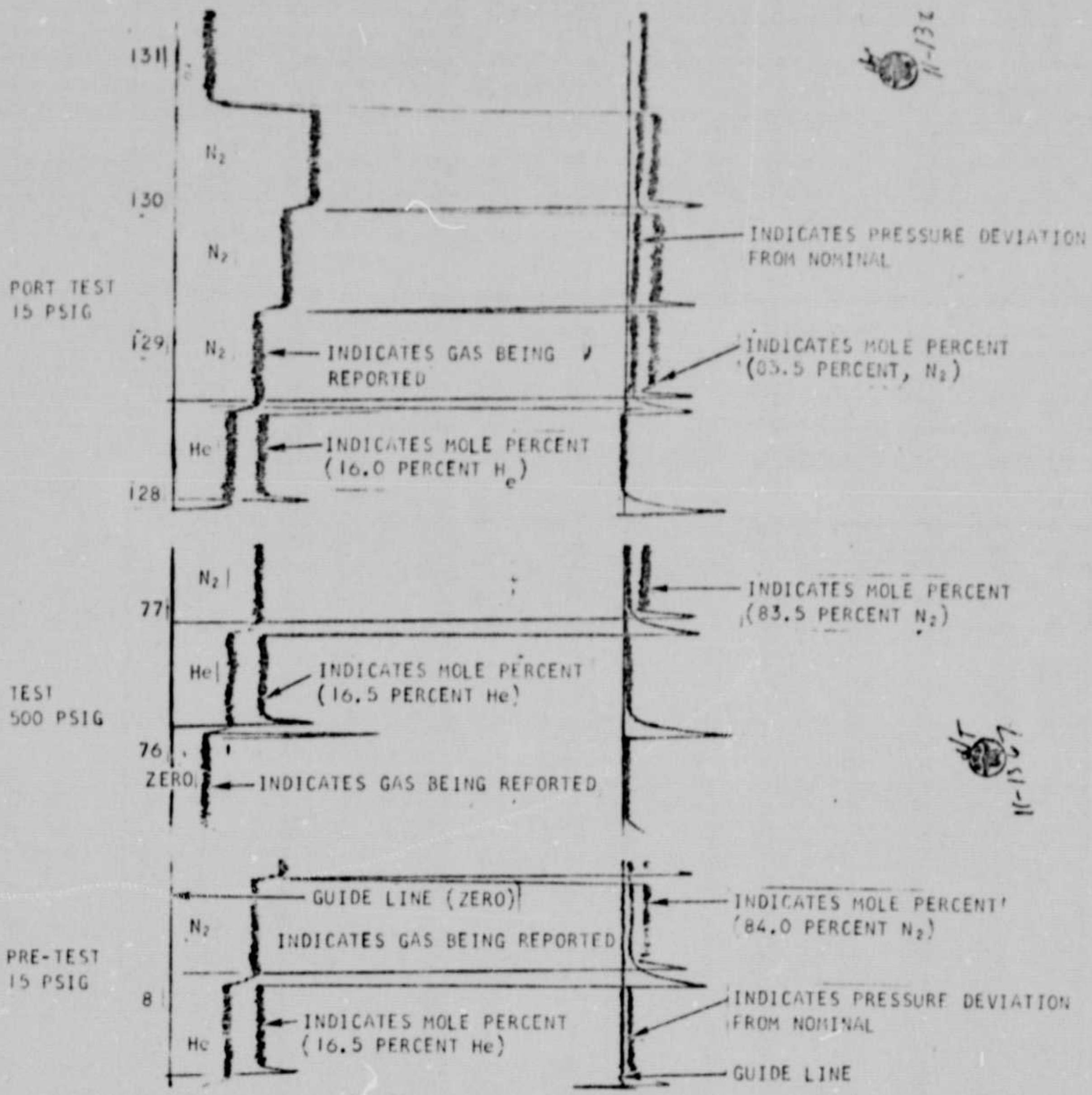

Figure 3.1- . Record of Mach 3 Test of Gas Sampling Subsystem

ORIGINAL PAGE IS OF POOR QUALITY

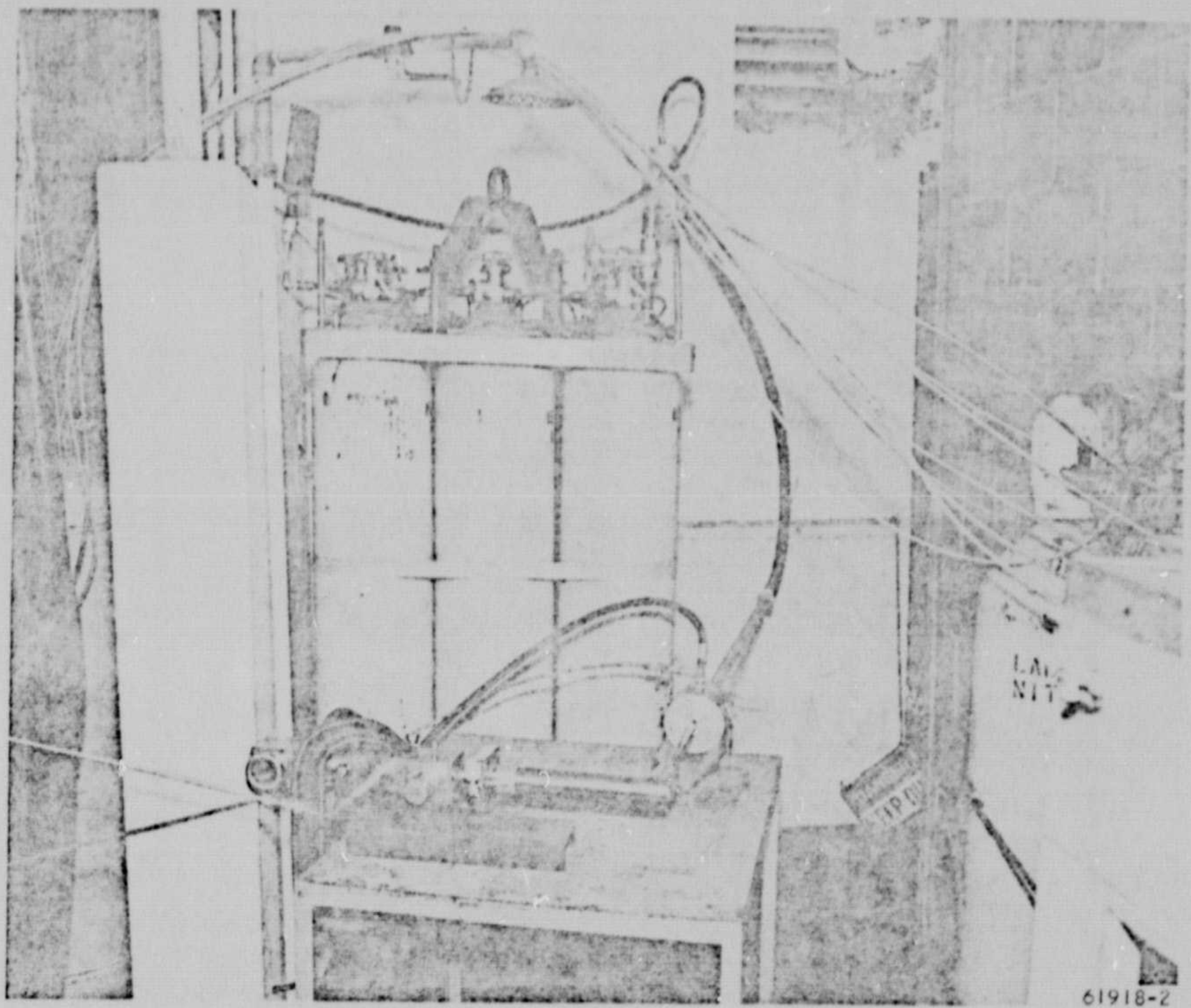

Figure 3.1-7. Probe Tip Inserted in Supersonic Nozzle

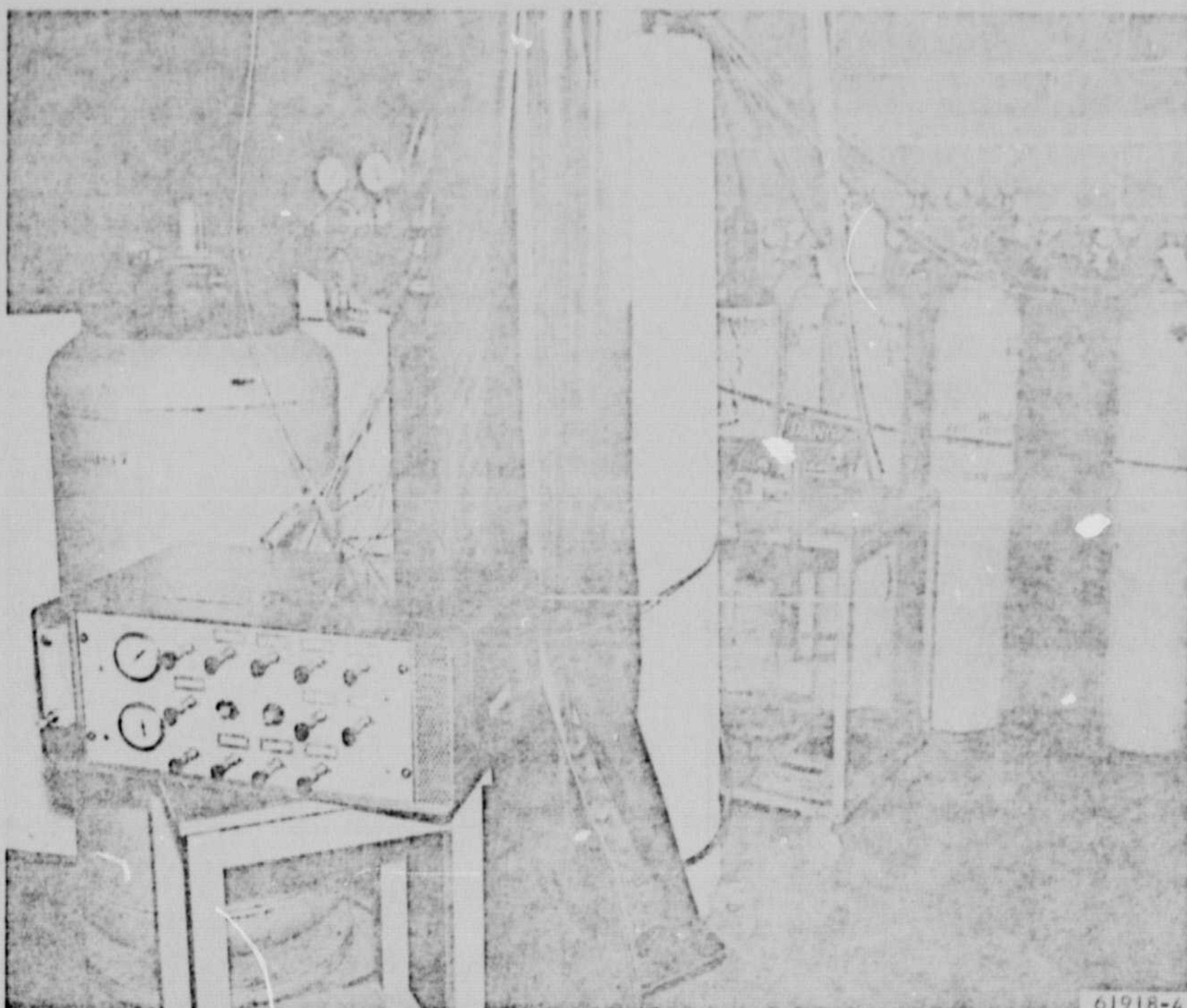

Figure 3.1-8. Combustor Calibration (Scani Valve)

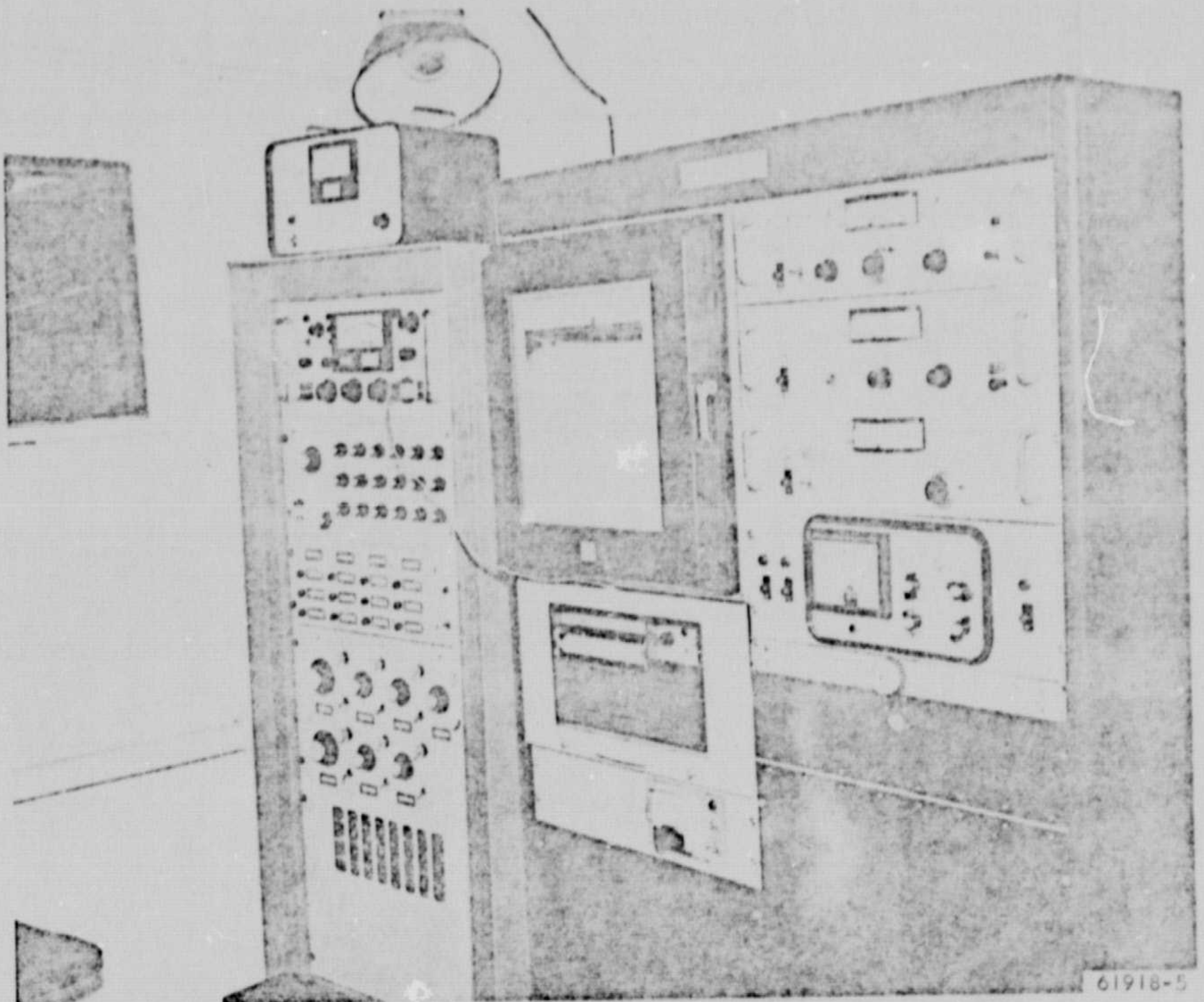

Figure 3.1-9. Auxilliary Cabinet and Mass Spectrometer

ORIGINAL PAGE IS
OF POOR QUALITY

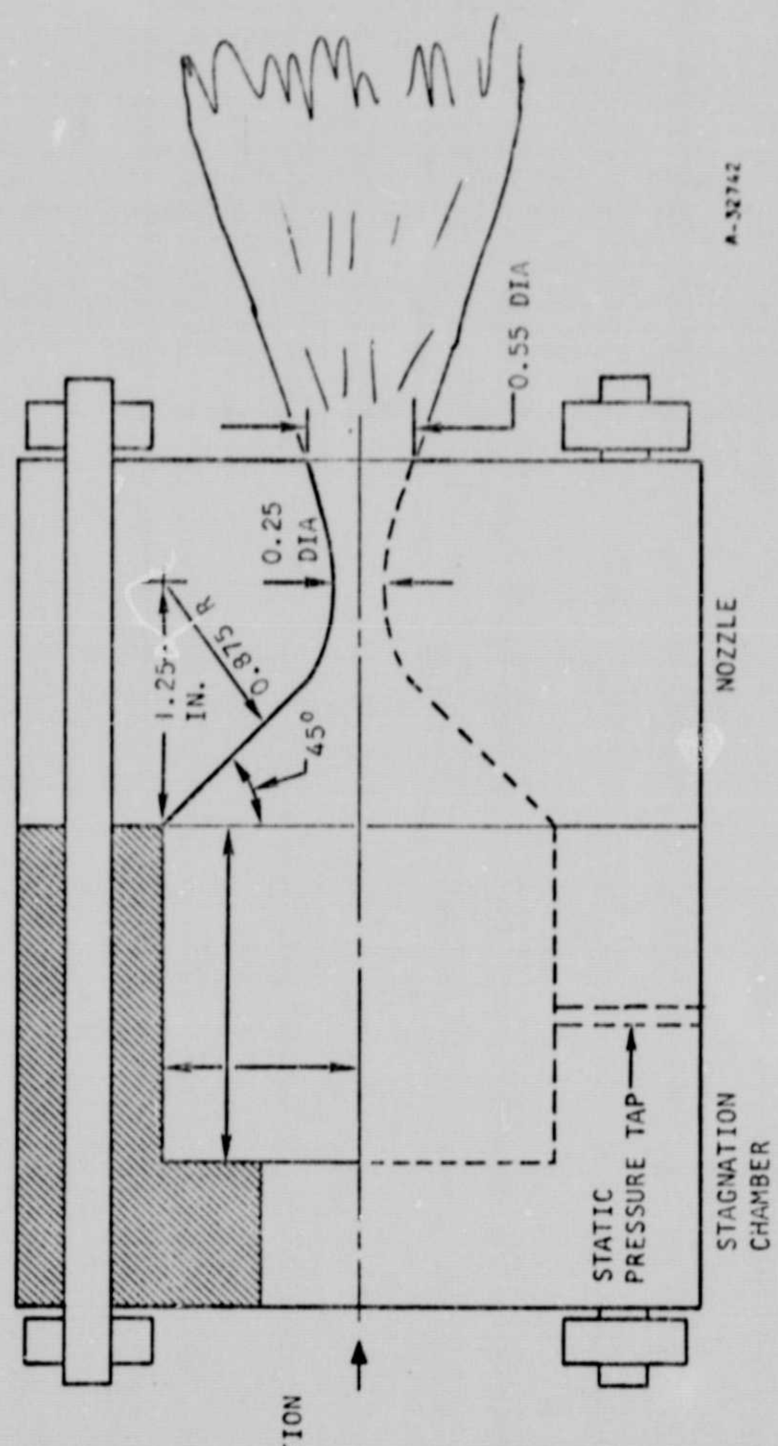

Figure 3.1-10. Mach 3 Nozzle Details (Material: Aluminum)

99.5 and 100.5 percent. The vendor only analyzed for He and a check for totals equaling 100 percent is not possible. This test compares the analysis of the gas when sampled under static and dynamic conditions.

Test results show that the analyses taken under the two conditions are the same, ±1/2 percent. The drift of the total system for this run of 2 min is 1 percent of full scale. This drift rate is about 10 times the rate that normally occurs.

The significance of the test is that it shows the gas analysis subsystem is capable of sampling supersonic gas flow and indicating that the composition is the same as that when a sample is taken at static conditions (which it should be). This applies to the particular gas sample used which was a molecularly mixed sample (molecules of helium are evenly dispersed throughout the nitrogen). The test showed that the pressure at the gold leak could adequately be controlled and the type of record which will be taken during the combustor tests is easily reduced to mole percent (or volume percent).

Filters were installed in the inlet system to prevent particles from fouling the Scani-valve switch or plugging the inlet capillary. Two filters were used. One filter was located immediately upstream of tube No. 4 (0.062 in. ID, Table 3.1-1) and downstream of the 3.0 psig relief valve. One filter was located immediately upstream of tube No. 7 (0.009 in. ID, Table 3.1-1). Both filters are photo-etched-stainless-steel sheets with 0.006 in. dia holes. The filters were placed flat against the end of a 1/4-in. tube and held in place when the tube was installed in the swagelock fitting.

In the event the inlet capillaries become plugged during operation by particles entering the probe from the gas stream, the location of the plugging will be indicated by relief valve not discharging gas to the atmosphere when the probe is pressurized.

A switch has been installed on the mass spectrometer to allow operation in any one of the following modes of operation:

(a) Peak selector not used (standard operation of mass spectrometer). Output recorded on

    (1) Ink pen recorder

    (2) Light beam recorder

(b) Peak selector used. Output recorded on

    (1) Ink pen recorder

    (2) Light beam recorder

3.2 GAS SAMPLING/TOTAL PRESSURE PROBE

3.2.1 Problem Statement

A device is needed to collect and distribute a sample of gas from the internal supersonic flow field of a hypersonic ramjet engine. The constituents of the sample must be truly representative of the gas stream sampled. The device must preserve the atomic balance of the constituents of the collected sample. The operating environments for this device include temperatures up to approximately 5800°R, velocities of approximately 3500 fps, an oxygen rich atmosphere, and the effluent gases of an oxygen-hydrogen burner. The device must be suitable for installation and use in both a fixed and traversing mode in a variety of test configurations associated with a hypersonic ramjet engine and component test program.

3.2.2 Topical Background

In order to determine oxygen-hydrogen combustor performance and determine how it is influenced by the injector geometry, jet penetration, and spreading, the mixing of the effluent gases must be ascertained at several points in the combustor with a probe. The probe must not be too large or it will block the combustor flow and choke it. The probe and its support must also be cooled in order to have sufficient life.

The gas mixture will be sampled during component and engine tests. The main objective will be to determine the mixing efficiency of the hydrogen fuel and the airstream. Accordingly, it will be necessary to determine the atomic balances to evaluate the extent of mixing. This approach is based on the consideration that the combustor performance is mixing limited in the supersonic combustion regime of greatest interest.

3.2.3 Overall Approach

It is difficult to get gas samples from a supersonic H_2 and air combustor. Cooling requirements for the probe and its support, plus the necessity for providing a coolant return so that no additional H_2O is added to the combustor flow dictates a complex design. Other major problems include capturing a truly representative sample of the combustion gases from any desired point in the combustor and preserving its composition while transporting it to a mass spectrometer for analysis.

In order to capture a representative sample of the gas stream, the detached bow shock, which exists around the leading edge of any body immersed in a supersonic stream, must be attached to the probe inlet. This prevents segregation of the sample due to inlet spillage and deflection of the lighter mass particles away from the inlet that would occur in the subsonic region behind the shock. The problem of preserving the composition of the sample is limited to preserving its atomic balance of H_2, N_2, O_2, and H_2O. No attempt will be made to analyze for any molecular species since the equilibrium of the species cannot be frozen when it enters the probe and would be subject to change since it might not be completely combusted. To preserve the atomic balance, the water vapor in the sample must not be allowed to condense on the walls of the probe or tubing transporting the sample to the gas analyzer.

With the above requirements and constraints, a preliminary design for a gas sampling probe was made and analyzed to ensure adequate cooling, structural integrity, ease of fabrication, and satisfactory aerodynamic performance.

3.2.4 Analytical Design

No further design analysis was required or performed during this reporting period.

3.2.5 Design Effort

The usefulness and capability of the gas sampling probe was increased to include stream total temperature measurement. This was accomplished by means of the calorimetric technique.

The application of this feature included the addition of a Daniels-type flow measuring section near the base of the vertical support tube to measure gas sample flow rate and provisions for measuring coolant flow rate and temperature rise.

Another design feature added to the probe is the provision for measuring stream static pressure. When combined with the total pressure measuring capability, the static pressure measurement, with proper calibration, will allow the determination of stream Mach number. The stream static measurement is taken by means of a wall tap through the outer tube just behind the transition from the tapered section of the straight circular section near the probe tip. This zone is most desirable for its insensitivity to Mach number (Reference 5.)

3.2.6 Manufacturing

Primary effort during this reporting period has been directed toward the fabrication of the gas sampling probe and the resolution of minor brazing problems in the sequence of assembly operations. Figures 3.2-1 through 3.2-3 show most of the major parts and subassemblies, with the exception of the gas flow measuring section and back pressure regulator valve.

3.2.7 Testing

Certain preliminary tests have been performed on the gas sampling probe to date. These tests have included, in part, leak, proof-pressure, and flow tests to determine pressure drops in the cooling system. The results of the test show that the probe will pass 1.54 gpm at 200 psi pressure drop; the predicted flow was 2.0 gpm at 200 psi pressure drop. In addition, system tests were performed to verify the ability of the probe to capture a representative sample of gases from a supersonic stream of gases flowing at a known mixture ratio and to determine operating characteristics and sample transport times of the overall gas analyzing system. These test verified the probe's ability to capture a representative sample of molecularly mixed gases flowing at supersonic velocities.

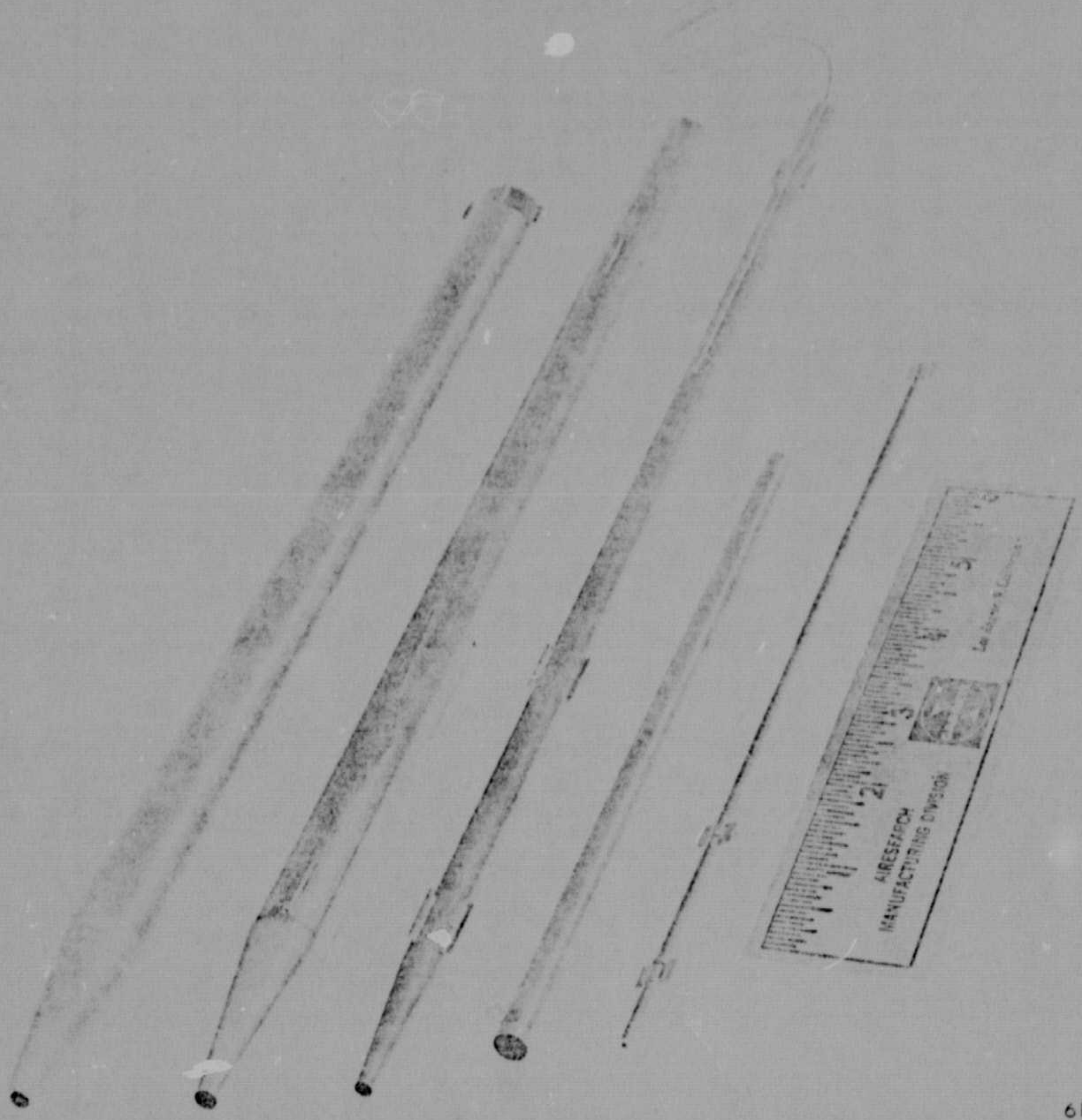

61670

Figure 3.2-1. Probe Sting Assembly

ORIGINAL PAGE IS
OF POOR QUALITY

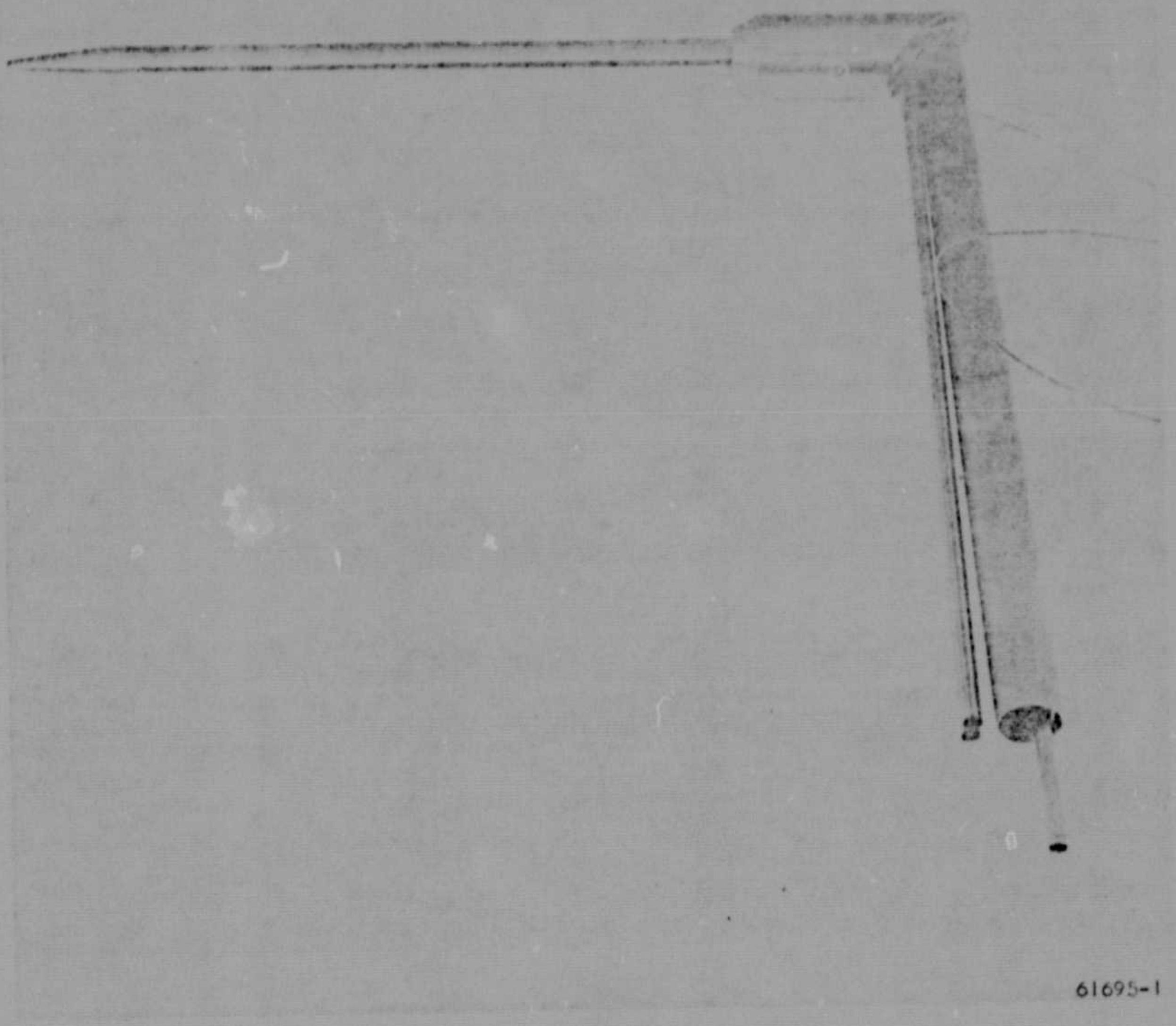

ORIGINAL PAGE IS
OF POOR QUALITY

Figure 3.2-2. Probe Tube Assembly

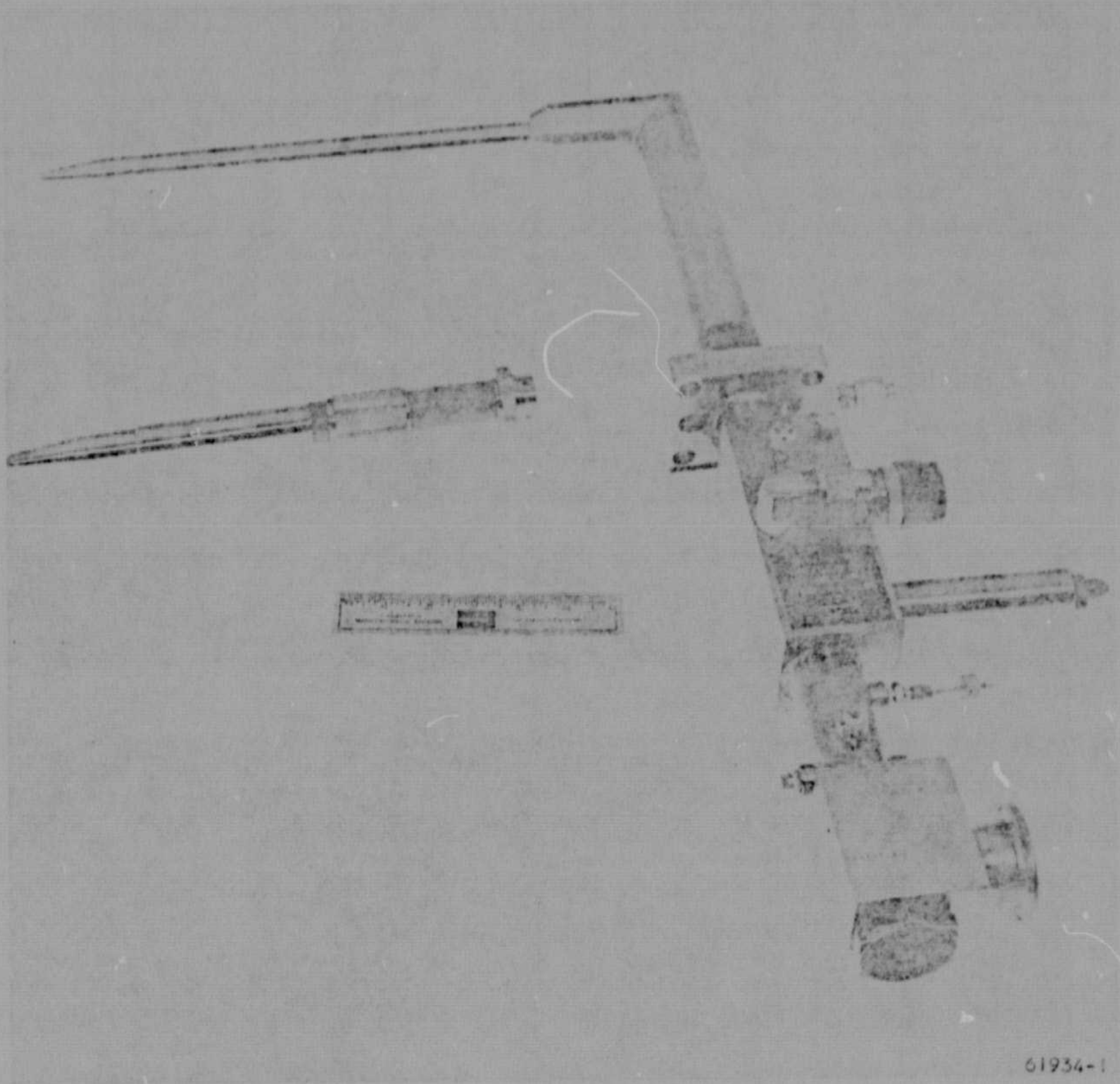

Figure 3.2-3. Gas Sampling Probe and Sting Protective Cover for Large-Scale Combustor Test Rig Application (P/N 981055-1)

ORIGINAL PAGE IS
OF POOR QUALITY

Figure 3.1-7 show the test setup used for the system tests in which the probe tip was exposed to a supersonic stream of ambient temperature gases in a known mixture ratio.

3.2.8 Future Action

Fabrication of the detailed parts and assembly of the backup probe will continue. Development tests to demonstrate mechanical integrity of the probe, adequate cooling, freedom from flutter, and verification of tip design will be performed. Calibration tests of the probe to determine the backpressure required to attach the bow shock over the required operating range of stream Mach numbers and calibration tests of the entire gas analyzing system will be performed. Calibration tests of the calorimetric total temperature measuring technique will also be performed.

4.0 TEMPERATURE MEASUREMENT SUBSYSTEM

The temperature measurement subsystem consists of the total temperature thermocouple and the double-sonic orifice total temperature probe. The total temperature thermocouple is discussed in Paragraph 4.1 and the double-sonic orifice probe is discussed in Paragraph 4.2.

4.1 TOTAL TEMPERATURE THERMOCOUPLE

4.1.1 Problem Statement

The objective of the total temperature thermocouple program is the development of a thermoelectric device to determine engine exhaust temperatures. The major areas of concern encompass the response, accuracy, and life of the device under severe exhaust flow conditions. These conditions cover a wide span of combustion modes in which the exhaust environment may range from a highly oxidizing atmosphere to one that is reducing or oxygen lean. Two fundamental problems exists:

(a) Thermocouple materials ideally suitable for the task are not available. Available thermocouple materials have a limited life in such a hostile operating environment and improved models are desired.

(b) Thermocouple uncertainty errors associated with the hot gas probe heat transfer mechanisms during the variable gas flow conditions are intolerably large and methods are required to reduce them to lower values.

4.1.2 Topical Background

Investigations so far point to the tungsten on tungsten and 26 percent rhenium combination as having the best overall characteristics suitable for the HRE task.

Ir/Ir Rh combinations, which can operate in oxidizing environments for longer periods show promise in applications where large known and assigned systematic radiation and conduction errors are considered for purposefully lowering the actual junction temperature.

4.1.3 Overall Approach

The total temperature thermocouple task is one of combining materials and developing fabrication techniques to assure sufficient probe life for the application. This approach must consider the necessity of certain forced tradeoffs of objectives due to the severe operating environment for the sensor.

A test facility for the thermocouple development program is available. The following approximate gas temperatures can be obtained with the energy available for sensor testing: 5600°F with an oxygen and hydrogen combination, 4700°F with a combination of hydrogen and air; and over 5600°F with an oxygen and acetylene combination. The gas mixtures can be controlled to permit a broad range of temperatures and conditions. Supporting equipment includes strip chart recorders, a radiometer, an optical pyrometer, and other temperature measuring equipment. Although this facility cannot duplicate all the operational engine conditions which the probe will encounter, it does provide the means to subject sensors to heat fluxes and temperature levels similar to those encountered in acutal service.

4.1.4 Overall Status

During the past quarter AiResearch recommended that development of an exit total temperature probe be limited to completion and evaluation of the double sonic orifice probe under construction, and that the use of this probe be limited to the inlet total temperature for the control system requirements. Justification for this cessation of development work on probes for measuring the exit total temperature is based on the necessity for extreme accuracy (0.1 percent) in this measurement for determining equivalent chemical efficiency of the combustion process.

The NASA reserved concurrence with this recommendation pending a comprehensive measurement analysis of all engine parameters and a detailed evaluation of the work performed to date on the exit temperature probe. Such activity is in process and will be reported in the next quarterly report.

4.2 DOUBLE SONIC ORIFICE TOTAL TEMPERATURE/PRESSURE PROBE

4.2.1 Problem Statement

Devices are needed to measure the total temperature and total pressure in the internal supersonic flow field of a hypersonic ramjet engine. These devices must be able to operate in a temperature of approximately 5800°R, a high velocity, approximately 3500 fps, oxygen rich atmosphere, and the effluent gases of an oxygen and hydrogen burner. These devices must be suitable for installation and use in a variety of test configurations for a hypersonic ramjet engine test program.

4.2.2 Background

In order to determine combustor performance and how it is influenced by injector geometry, jet penetration, spreading, and mixing, total temperature and total pressure at several points in the combustor must be measured while the engine is operating. The probe concept and size are affected by the necessity of keeping the combustor duct unblocked so it will not become choked. Also, the probe must be cooled to attain sufficient life to make the tests.

Obtaining temperature and pressure measurements from a supersonic oxygen and hydrogen burner involves many factors. The probes and supporting systems must be cooled. The coolant selected must be compatible with the test facility, installation, and test objectives. In the cases discussed here, the test objectives have necessitated circulation of the coolant through the probe. Further, the test facilities and configurations using the probe will allow the use of two alternate coolant fluids, hydrogen and water.

4.2.3 Overall Approach

One gas aspirating cooled probe design will be tested and fabricated. The probe shown in Figure 4.2-1 will be used in the Phase II segmented combustor test rig. The probe is internally cooled to a temperature compatible with structural requirements and the aspirated air is cooled to about 2300°R or less.

The probe detects the total temperature by two independent methods: the two-sonic orifice method, and the calorimetric method. The working principles of these methods are described in Reference 5. Both methods of temperature measurement are incorporated in the same physical probe. For evaluating the total temperature from the two-sonic orifice method, measurements of the total pressure in the inlet nozzle and total pressure and temperature in the second nozzle are required. For the calorimetric method, total pressure and total temperature in the second nozzle, mass flow rate of the coolant, the inlet and outlet temperature of the coolant, and a check valve for stopping the gas aspiration to take tare measurements are required.

Since the flow of gas through the probe must be deadheaded to make a tare measurement of heat flux, due to the external free stream flow around the probe, a pressure transducer will be used to measure total pressure. The free stream total pressure may then be computed by using the Rayleigh equation as solved for a real gas. It is possible therefore, to make three determinations with the probe; total temperature by the double-sonic orifice method, total temperature by the calorimetric method, and total pressure.

4.2.4 Analytical Design

No further design analysis was performed during this reporting period. An error analysis was initiated to determine the expected error in the final value for free stream total temperature and will be published in a separate document

4.2.5 Design Effort

A design feature added to the double sonic orifice probe is a provision for measuring stream static pressure similar to the gas sampling probe application described in Section 3.2. When combined with the total pressure measuring capability the static pressure measurement, with proper calibration, will

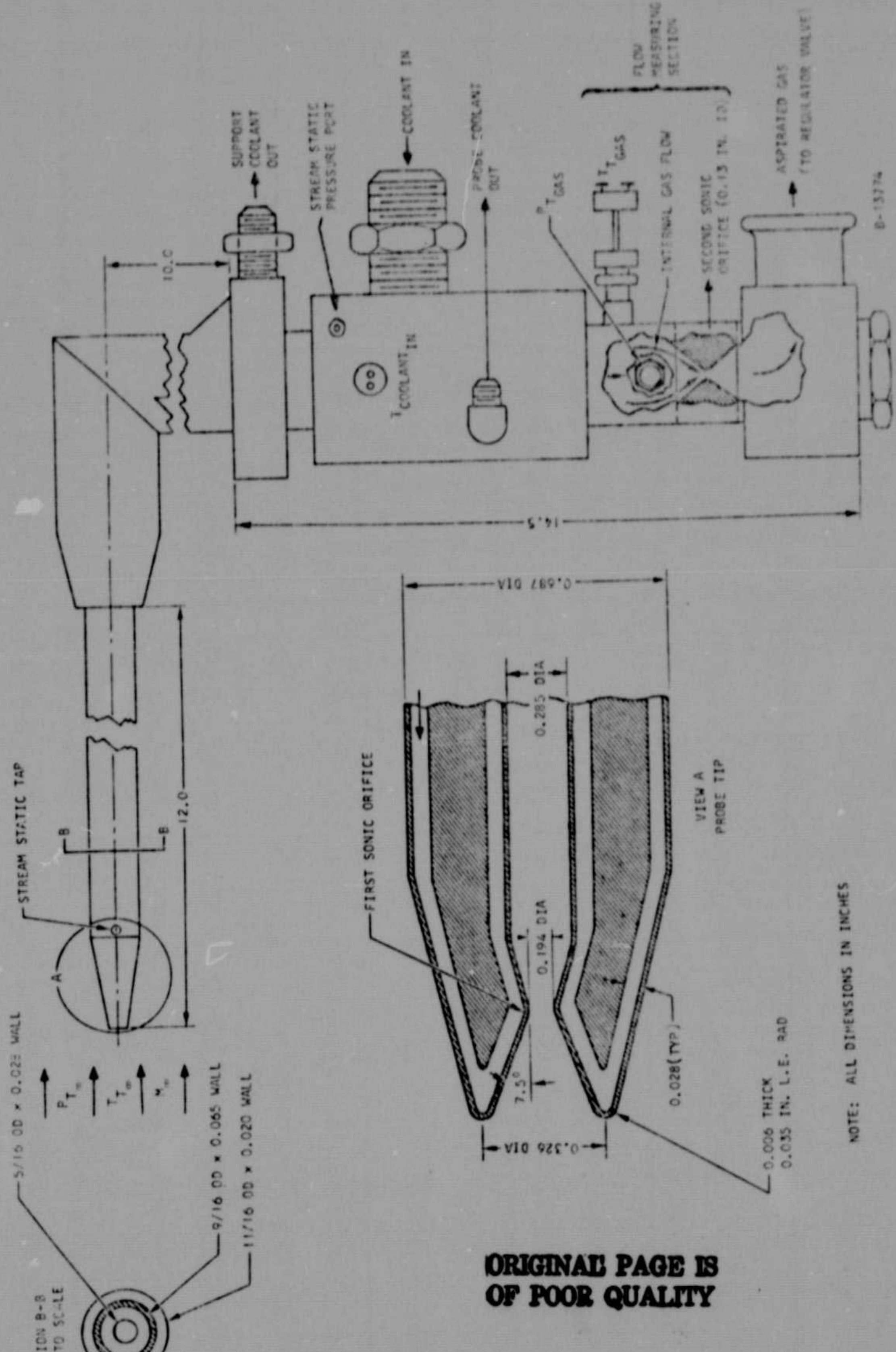

Figure 4.2-1. Double Sonic Orifice Total Temperature Probe (Segmented Combustor Application)

ORIGINAL PAGE IS OF POOR QUALITY

allow the determination of free stream Mach number. The stream static measurement is taken by means of a wall tap through the outer tube just behind the transition from the tapered section to the straight circular section near the probe tip. This zone is most desirable for its insensitivity to Mach number (Reference 5.)

4.2.6 Manufacturing

The double sonic orifice total temperature/pressure probe is fabricated entirely of corrosion resistant steel. All detail components are fabricated and joined by conventional techniques.

4.2.7 Future Action

Fabrication of detail parts and assembly of the probe will continue toward a timely introduction into the combustor segment test program for probe evaluation and development. Tests to demonstrate mechanical integrity of the probe, adequate cooling capability, and freedom from flutter will be performed. Calibration tests of the double-sonic orifice and calorimetric temperature measurement features under simulated combustor conditions will also be performed after completion of the development tests.

5.0 ENGINE TEMPERATURE MEASUREMENT SUBSYSTEM

The temperature measuring system as contemplated at the present time will employ Chromel/Constantan and Geminol P&N thermocouple materials. The Chromel/Constantan will be used in the control circuits where maximum sensitivity is required over limited ranges. The Geminol "P and N" will be used for recording information which is applicable to the full range requirements for the PCM System used onboard the X-15. It is not contemplated to use resistive sensing devices in the instrumentation system.

5.1 BASIC SENSOR CONSTRAINTS

Constraints placed upon the temperature sensor selection by the engine fabrication procedures generally limits the basic selection to the thermocouple type sensor. Metal temperature sensors must be capable of withstanding the temperature excursions encountered during the several braze cycles the engine will go through. Experience has shown that resistive devices which are compatible with this type of installation cannot be subjected to brazing cycles of 2000°F without extreme calibration shifts. Physically the thermocouple sensor is the only type which will readily adapt to the hot skin surface temperature measurement configuration. Most measurand locations within the engine require that the sensors be installed during the engine assembly. To retain gas and coolant temperature leak integrity the sensor must either be installed during engine build up or if after build up, where accessible, in sensor wells which make the measurement incompatible with the desired time constant requirements of the system. In view of the fabrication constraints imposed on the measuring system, the initial effort in the subsystem temperature measurement investigation has been with the adaptibility of the thermocouple to satisfy the measurand requirement. In general, the flight engine is the design goal, with the temperature instrumentation compatible with the PCM input requirements.

5.2 THERMOCOUPLE MATERIAL

The thermocouple material has been selected to satisfy the range demanded by the readout system aboard the aircraft. Two avenues were considered to meet the above requirements.

(a) Select a thermocouple material and attenuate the output by electrical means to satisfy the range requirement. This approach will require an attenuation circuit for each channel.

(b) Select a thermoelectric material combination which will closely fit the full scale output of the temperature ranges desired.

Homogeniety and temperature stability characteristics of Geminol P&N* wires are better than the Chromel/Alumel pairs. This combination has an EMF vs Temperature output which is compatible with the signal conditioning requirements for the PCM equipment.

Limited knowledge was available for the combinations output in the cryogenic temperature region. Calibration checks to the liquid hydrogen point indicated no EMF reversals or unusual characteristics negating the possible use in this program. The temperature range is from 40°R (-420°F to 1800°R.

5.3 REFERENCE JUNCTION

The temperature instrumentation system including the reference junction subsystem is grouped into four basic regions, each region to satisfy the temperature instrumentation reference requirements in that portion of the engine. This approach makes it possible to reference the thermocouple circuits and have sensor output leads without having to cross interface disconnects which are potential thermoelectric error sources in areas of large temperature gradients. As shown in Figure 5.3-1 the power supply is accessible via the aft end of the nozzle section.

5.4 INPUT LEVELS

The PCM system aboard the X-15 aircraft requires that a ±0 - 15 millivolt or ±0 - 5 volt full scale signal shall be available for recording of data information. Ranging for maximum resolution must be conditioned to meet these input requirements. All conditioning from the temperature measuring system is anticipated to be 0 ±15 millivolts to the PCM. The use of any preamplification circuitry is not planned for the temperature measuring system.

5.5 ACCURACY

Figure 5.3-2 shows the error band expected for flight version, considering the three basic errors of the system: the PCM, the Reference Junction, and the thermoelectric deviation of the thermocouple. Accuracy of this system rapidly falls out of requested tolerances below 350°R, mainly due to the PCM and Reference junction errors. The wide excursion of ambient temperature range to which the reference junction is exposed accounts for an equivalent 3σ error to 65°F in the cryogenic regions. This is also true with the errors associated with the PCM. Three σ errors for this system approach 100°F at the extreme cryogenic temperature.

*Geminol P&N is a Nickle Silicon (negative) versus a Nickel Chromium (positive) thermocouple combination and is manufactured by Driver Harris Company of Harrison, New Jersey.

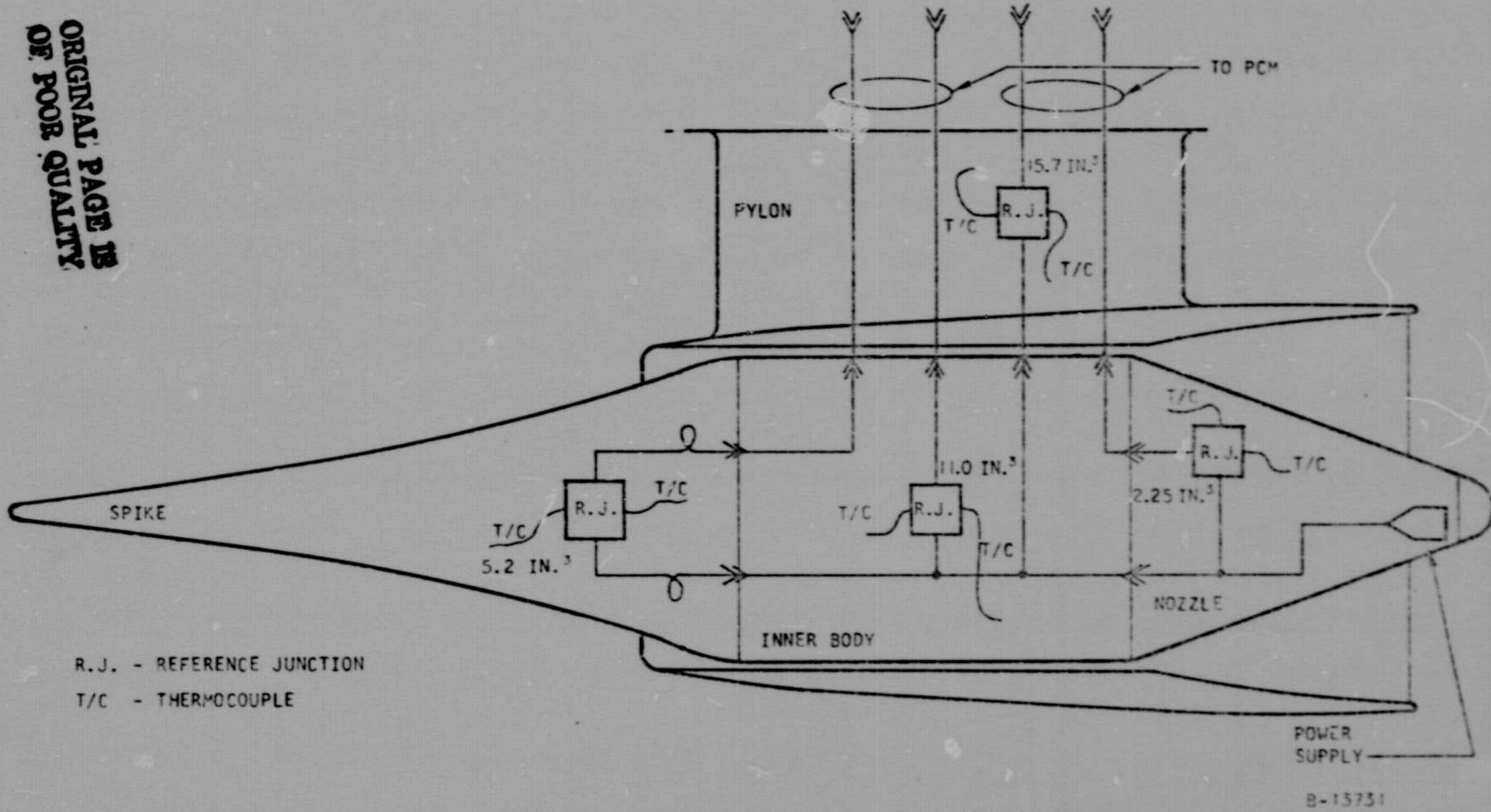

R.J. - REFERENCE JUNCTION

T/C - THERMOCOUPLE

Figure 5.3-1. Thermocouple System, HRE Flight Engine

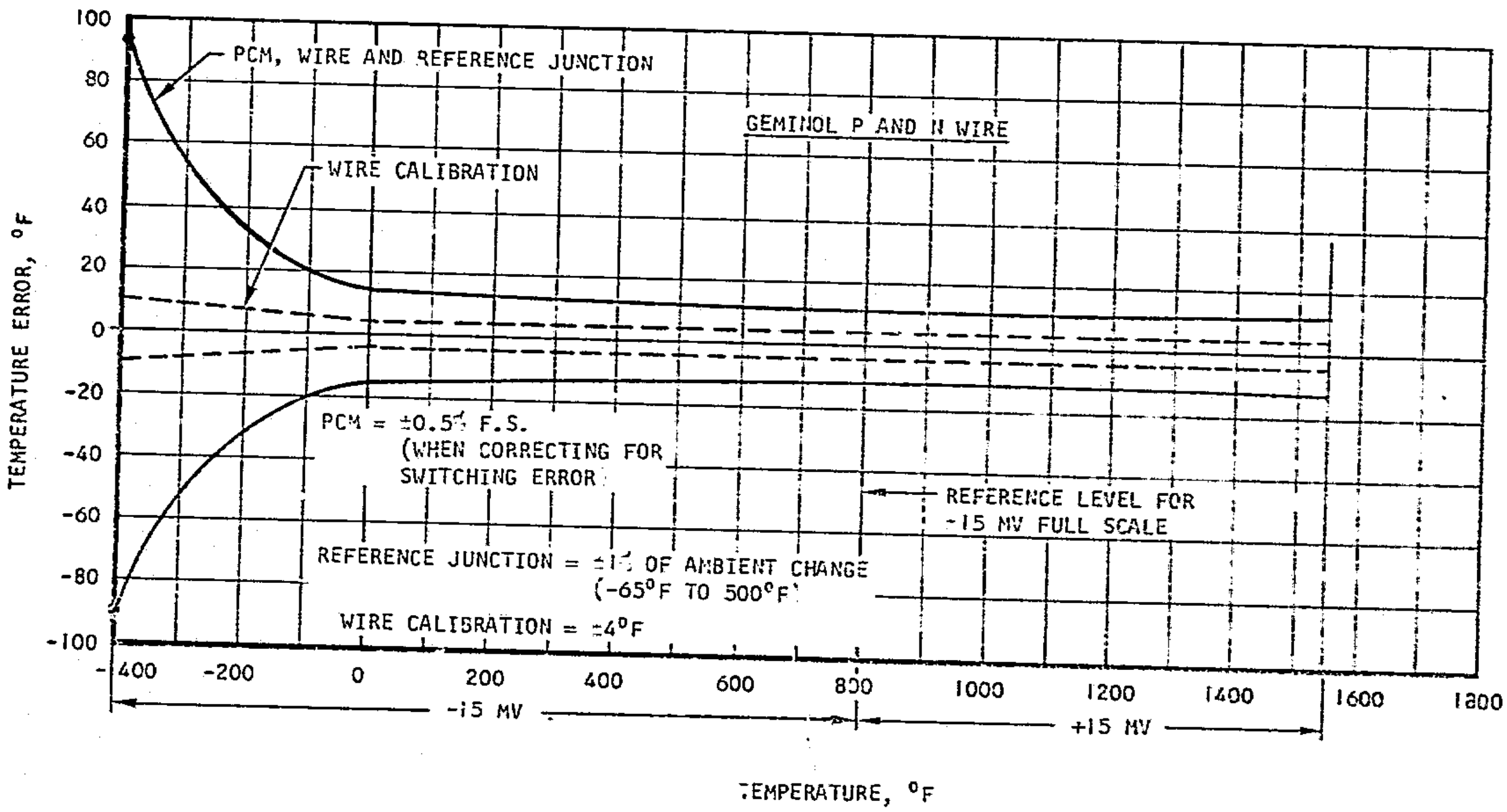

Figure 5.3-2. Temperature Error: RSS of 3σ Constituents Approximate Range -420°F to +1550°F

5.6 INSTRUMENTATION AND CONTROL INTERFACE

Consideration was given to the possible use of the same temperature sensors for control and readout. This approach was dropped because of possible interface problems. The major drawbacks to the approach are listed below.

(a) Control systems sensors must be ungrounded.

(b) Range is not compatible

(c) Possible system feedback between control and instrumentation circuits when in parallel affecting the reliability of the systems.

(d) Time constant requirements different.

(e) Sensor Sensitivity requirements not compatible.

To satisfy the circuit requirements, individual sensors and circuitry compatible to each system requirements are to be used with the duplication of the applicable sensors in discrete areas.

5.7 RESISTANCE SENSORS

The apparent large errors associated with thermocouple sensors in the cryogenic areas, prompts one to look to other sensor types which may have better low temperature characteristics and are compatible to the total instrumentation plan. Although the brazing cycle temperatures the engine encounters during buildup (Paragraph 5.1) will generally rule out the resistive devices, both semiconductor and metal.

5.8 ERROR REDUCTION

Review of the errors associated with the Flight Engine installation indicate the major portion of the total error is associated in two areas of the system.

(a) PCM Data Recording

(b) Compensating Reference Junction (due to ambient temperature variations)

An appropriate reduction of the overall error can possibly be reduced by further consideration and effort in these areas.

One approach with the PCM system can be an error analysis associated with the time and environmental history of the total system, thereby reducing some of the random errors to systematic errors capable of correction to the system. Another approach which may be possible is to time share during flight a set of precise voltage inputs to the PCM System using this as a calibration reference for each channel of information. These areas will require further investigation since it is in this category that a large reduction of the over all system error appears possible.

In the thermocouple circuit the Reference Junction error associated with the anticipated large ambient temperature changes are responsible for a major part of the overall inaccuracy of the measurement.

Several possible approaches may be taken to reduce the error.

(a) Stabalize the reference junction body so that it does not see the large temperature excursion. By this approach two things are accomplished which will reduce the error.

(1) The percentage error which is proportional to the amount of temperature excursion will be reduced.

(2) The limited ambient excursion of the reference will allow a smaller percentage error factor to be applied. Instead of 1 percent of the ambient excursion a 0.5 percent factor would be applicable.

These approaches call for a basic refinement of the existing system. Each will add to the complexity of the system and would be more beneficial in the readout of the measurements in the cryogenic ranges. Ground engine tests may indicate that the need or total range on each channel is not required and channels incorporating the refinements may be selectively chosen for the flight engine.

References

1. Engineering Staff, "Phase I Conceptual and Preliminary Design," AiResearch Report No. L-9544, September 27, 1965.

2. Engineering Staff, "Phase I (Appendix A) Ramjet Preliminary Design Report (U) Vol. II", AiResearch Report No. AP-66-0168-2.

3. Statement of Work, Phase IIA, L-4947B.

4. Engineering Staff, "Aerodynamic and Engine Performance Analysis - First Interim Technical Data Report", (U) AiResearch Report No. 67-2631, pp. 5 and 6.

5. Volluz, R. J., "Handbook of Supersonic Aerodynamics, Section 20", NavOrd Report 1488, Vol. 6, January 1961.